

**Figure 3.** Periods of cyclosporin treatment and remission. Cyclosporin treatment was ceased at the time point when 75% or more reduction in the Psoriasis Area and Severity Index score (PASI 75) was achieved. The period of cyclosporin treatment in each course (1st to 5th courses) was calculated and analyzed by Kruskal–Wallis ANOVA and Mann–Whitney *U*-test with Bonferroni correction.

**Doses of topical corticosteroids and vitamin D<sub>3</sub> analogs**

The doses of topical corticosteroids used for psoriatic lesions at 0 (just before CyA therapy), 12 and 48 weeks after commencement of CyA were gradually declined from 75.8 ± 37.2 to 30.7 ± 8.28 g/month, and retained at week 96 (Fig. 4a). The mean dose of corticosteroids 1 year after initiation of CyA was significantly decreased ( $P = 0.006$  [Kruskal–Wallis ANOVA];  $P = 0.28$ , 0 vs 12 weeks;  $P = 0.023$ , 0 vs 48 weeks; and  $P = 0.0032$ , 0 vs 96 weeks [Mann–Whitney *U*-test with Bonferroni correction]). No significant changes in the dose of topical vitamin D<sub>3</sub> analogs were noted (Fig. 4b), but the post-1-year dose also tended to be declined ( $P = 0.063$ ).

**Patient satisfaction**

Evaluation of patient satisfaction using a 3-point rating system revealed satisfaction scores were 1.07 ± 0.26, 2.43 ± 0.63 and 2.62 ± 0.35 at weeks 12, 48 and 96, respectively. A significant increase in the satisfaction score from baseline was seen during the course of the study ( $P = 0.011$  [Kruskal–Wallis ANOVA];  $P = 0.00013$ , 12 vs 48 weeks; and  $P = 0.00005$ , 12 vs

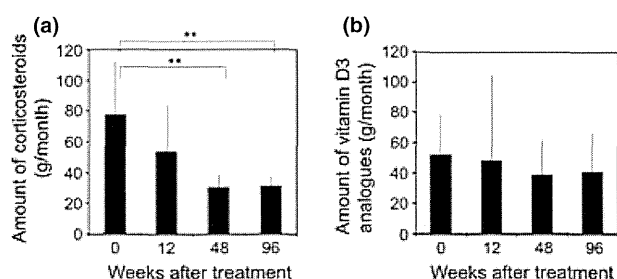


**Figure 4.** Amounts of corticosteroid and vitamin D<sub>3</sub> ointments used in the patients. Topical corticosteroids and vitamin D<sub>3</sub> were allowed in this study. The applied dose of corticosteroids and vitamin D<sub>3</sub> ointments were monitored monthly. Each dose was calculated and analyzed by Kruskal–Wallis ANOVA and Mann–Whitney *U*-test with Bonferroni correction. \* $P < 0.05$ , \*\* $P < 0.01$ .

96 weeks [Mann–Whitney *U*-test with Bonferroni correction]; Fig. 5a). Self-administered PASI scores significantly decreased from 12.5 ± 8.5 to 0.84 ± 0.05 ( $P = 1.12 \times 10^{-14}$  [Kruskal–Wallis ANOVA];  $P = 0.033$ , 0 vs 12 weeks;  $P = 0.022$ , 0 vs 48 weeks; and  $P = 0.013$ , 0 vs 96 weeks [Mann–Whitney *U*-test with Bonferroni correction]; Fig. 5b).

**Adverse side-effects**

There were a total of 16 adverse events in 14 patients at week 12, two adverse events in two patients at week 48, and three adverse events in two patients at week 96. The adverse events included facial nerve paralysis, general fatigue, polyuria, tinea corporis, decreased serum immunoglobulin M, proteinuria, hyperlipidemia, hypertension, elevated levels of creatinine and blood urea nitrogen, and elevated total bilirubin. Ten patients were withdrawn from the study because of facial nerve paralysis, elevated creatinine, hyperlipidemia, proteinuria or general fatigue. These events resolved after cessation of CyA.

**DISCUSSION**

The present study showed that low-dose, intermittent CyA microemulsion therapy is effective and useful for the treatment of mild to moderate psoriasis. PASI 75 was achieved approximately 48 weeks after CyA therapy. Only 27.4% of patients required the second course of the therapy, and further CyA was unnecessary in these patients for approximately 3 months after achievement of remission. The third course of CyA was required in only 12 patients. As the adverse effect, one case of hypertension was observed.

Biologics have become a mainstay therapy for severe psoriasis,<sup>1</sup> which can induce dramatic skin improvement and improve patients' QOL.<sup>10,11</sup> However, the use of these agents requires monitoring for infections such as tuberculosis and pneumocystis pneumonia. In addition, the annual cost of biologics is relatively higher than other systemic therapies including CyA microemulsion. Furthermore, continuous treatment with

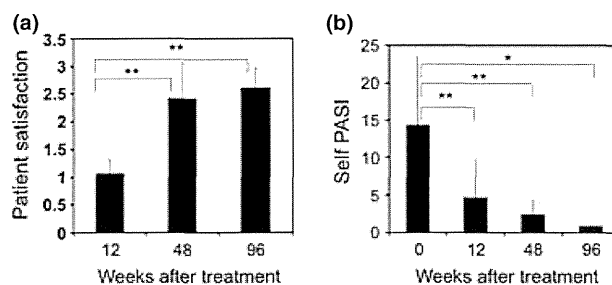


**Figure 5.** Patient satisfaction and self-administered Psoriasis Area and Severity Index (PASI) score. Patient satisfaction was evaluated at 12 weeks and 1 year after treatment, and on the last day of treatment using the following scores: 3, very satisfied; 2, satisfied; and 1, not satisfied. Self-administered PASI was used to assess quality of life. Each score was calculated and analyzed by Kruskal–Wallis ANOVA and Mann–Whitney *U*-test with Bonferroni correction. \* $P < 0.05$ , \*\* $P < 0.01$ .

biologics is required to maintain therapeutic effect and to avoid a loss of response.

Cyclosporin belongs to the second-line treatment for psoriasis and has been widely used for moderate and severe psoriasis.<sup>2</sup> This immunosuppressant can be used either continuously or intermittently depending on the patient's condition. Several studies have suggested that CyA serves as maintenance therapy in psoriasis vulgaris. Ohtsuki *et al.*<sup>3</sup> conducted a multicenter, randomized, controlled study to assess the long-term efficacy and safety of CyA for psoriasis using either a continuous or an intermittent regimen. In their study, the initial dose was 3–5 mg/day in both regimens, and patients in the continuous treatment group received 0.5–3 mg/day once remission was achieved. In the event of relapse, the dose was gradually escalated to 3–5 mg/kg per day until remission was obtained. In the intermittent group, the dose was tapered once remission was achieved and the drug was eventually ceased. The PASI score was decreased by more than 70% with no significant difference between the two regimens.

A study of daily versus intermittent application of high concentration tacalcitol ointment combined with low-dose CyA microemulsion was reported by Abe *et al.* in 2006.<sup>4</sup> Although patients in both groups showed significant improvement, patients in the intermittent application group were more satisfied, and intermittent topical therapy was associated with superior cost performance. The cost of low-dose CyA microemulsion with intermittent application of tacalcitol ointment was less than half of that of high-dose CyA microemulsion with daily application of tacalcitol. The same authors also reported a study of low-dose CyA preconcentrate (2.5 mg/kg per day) over 12 weeks in 2007.<sup>5</sup> The dose of CyA was reduced to 1.5 mg/kg per day and topical vitamin D<sub>3</sub> was commenced once PASI 75 was achieved. All patients showed improvement within 12 weeks, and 10 of 19 patients achieved over 75% reduction in PASI score. No adverse effects were noted during treatment.

In a randomized, controlled study, Shintani *et al.*<sup>7</sup> treated psoriatic patients with either 100 mg CyA emulsion once daily (group A) or 50 mg twice daily (group B). The improvement rate was 69.4% in group A and 73.4% in group B. PASI 75 and 90 were achieved in both groups with no significant difference at 12 weeks. Vena *et al.*<sup>8</sup> reported that a greater PASI reduction was achieved after combined therapy with low-dose CyA (2 mg/kg per day) and calcipotriol-betamethasone dipropionate ointment compared with CyA and emollient treatment in patients with moderate to severe plaque psoriasis.

Our study monitored psoriatic patients treated with CyA over a greatly longer period than the other studies. This study confirmed the efficacy of CyA in the treatment of psoriasis without the development of severe adverse effects. Repeated courses of CyA therapy improved psoriatic skin eruptions and well controlled the condition. The amount of topical corticosteroids was significantly reduced by repeated therapy, and the skin eruptions could be maintained by topical vitamin D<sub>3</sub> analogs. CyA-induced liver and kidney dysfunction may be avoided by using intermittent therapy. However, our study also showed that 10 patients withdrew because of their adverse

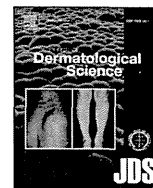
effects. Therefore, we should always use CyA carefully on patients with psoriasis.

Even for psoriatic patients under regular dermatological care, the QOL of patients with psoriasis vulgaris is comparable to that of patients with diabetes, coronary heart disease and cancer.<sup>12</sup> Currently, the PASI score and body surface area involvement are the most commonly used parameters in Europe for evaluating the clinical severity of psoriasis vulgaris.<sup>2</sup> PASI 75 is the benchmark used in clinical studies, and the majority of patients with PASI 75 experience improvements in QOL and in the Dermatology Life Quality Index. Despite the limitation of the open-label design, our present study suggests that low-dose, intermittent CyA microemulsion is efficacious with a favorable risk/benefit ratio.

**CONFLICT OF INTEREST:** None.

## REFERENCES

- 1 Cohen SN, Baron SE, Archer CB; British Association of Dermatologists and Royal College of General Practitioners. Guidance on the diagnosis and clinical management of psoriasis. *Clin Exp Dermatol* 2012; **37** (Suppl 1): 13–18.
- 2 Nast A, Boehncke WH, Mrowietz U *et al.* S3 – Guidelines on the treatment of psoriasis vulgaris (English version). Update. *J Dtsch Dermatol Ges* 2012; **10** (Suppl 2): S1–S95.
- 3 Ohtsuki M, Nakagawa H, Sugai J *et al.* Long-term continuous versus intermittent cyclosporin: therapy for psoriasis. *J Dermatol* 2003; **30**: 290–298.
- 4 Abe M, Syuto T, Hasegawa M, Sogabe Y, Yokoyama Y, Ishikawa O. Daily versus intermittent application of high-concentration tacalcitol ointment in combination with low-dose cyclosporin for psoriasis vulgaris. *J Dermatol* 2006; **2**: 108–111.
- 5 Abe M, Ishibuchi H, Syuto T, Sogabe Y, Yokoyama Y, Ishikawa O. Clinical usefulness and patient satisfaction for treatment with low-dose cyclosporin administration in patients with moderate psoriasis vulgaris. *J Dermatol* 2007; **34**: 290–293.
- 6 Hashizume H, Ito T, Yagi H *et al.* Efficacy and safety of preprandial versus postprandial administration of low-dose cyclosporin microemulsion (Neoral) in patients with psoriasis vulgaris. *J Dermatol* 2007; **34**: 430–434.
- 7 Shintani Y, Kaneko N, Furuhashi T, Saito C, Morita A. Safety and efficacy of a fixed-dose cyclosporin microemulsion (100 mg) for the treatment of psoriasis. *J Dermatol* 2011; **38**: 966–972.
- 8 Vena GA, Galluccio A, Pezza M, Vestita M, Cassano N. Combined treatment with low-dose cyclosporine and calcipotriol/betamethasone dipropionate ointment for moderate-to-severe plaque psoriasis: a randomized controlled open-label study. *J Dermatolog Treat* 2012; **23**: 255–260.
- 9 Warren RB, Griffiths CE. Systemic therapies for psoriasis: methotrexate, retinoids, and cyclosporine. *Clin Dermatol* 2008; **26**: 438–447.
- 10 Leonardi CL, Kimball AB, Papp KA *et al.* Efficacy and safety of ustekinumab, a human interleukin-12/23 monoclonal antibody, in patients with psoriasis: 76-week results from a randomised, double-blind, placebo-controlled trial (PHOENIX 1). *Lancet* 2008; **371**: 1665–1674.
- 11 Papp KA, Langley RG, Lebwohl M *et al.* Efficacy and safety of ustekinumab, a human interleukin-12/23 monoclonal antibody, in patients with psoriasis: 52-week results from a randomised, double-blind, placebo-controlled trial (PHOENIX 2). *Lancet* 2008; **371**: 1675–1684.
- 12 Rapp SR, Feldman SR, Exum ML, Fleischer AB Jr, Reboussin DM. Psoriasis causes as much disability as other major medical diseases. *J Am Acad Dermatol* 1999; **41**: 401–407.



## Induction of cytotoxic T cells as a novel independent survival factor in malignant melanoma with percutaneous peptide immunization



Toshiharu Fujiyama<sup>a,\*</sup>, Isao Oze<sup>b</sup>, Hiroaki Yagi<sup>a</sup>, Hideo Hashizume<sup>a</sup>, Keitaro Matsuo<sup>c</sup>, Ryosuke Hino<sup>d</sup>, Riei Kamo<sup>e</sup>, Shuhei Imayama<sup>f</sup>, Satoshi Hirakawa<sup>a</sup>, Taisuke Ito<sup>a</sup>, Masahiro Takigawa<sup>a</sup>, Yoshiki Tokura<sup>a</sup>

<sup>a</sup> Department of Dermatology, Hamamatsu University School of Medicine, Japan

<sup>b</sup> Division of Epidemiology and Prevention, Aichi Cancer Center Research Institute, Japan

<sup>c</sup> Department of Preventive Medicine, Kyusyu University, Japan

<sup>d</sup> Department of Dermatology, University of Occupational and Environmental Health, Japan

<sup>e</sup> Department of Dermatology, Osaka City University Graduate School of Medicine, Japan

<sup>f</sup> Imayama Shuhei Clinic & Lab, Japan

### ARTICLE INFO

#### Article history:

Received 5 February 2014

Received in revised form 3 April 2014

Accepted 5 April 2014

#### Keywords:

Percutaneous peptide immunization

Melanoma

Cytotoxic T lymphocytes

### ABSTRACT

**Background:** Malignant melanoma (MM) often shows multiple chemo-resistance, leading to poor prognosis of the patients. Therapeutic anti-cancer vaccination may be a feasible way to prolong the survival of patients. We have demonstrated that application of antigenic peptides via the tape-stripped, horny layer-removed skin, known as percutaneous peptide immunization (PPI), induces tumor cell-specific cytotoxic T lymphocytes (CTLs) in rodents and humans.

**Objective:** To evaluate clinical significance of PPI in advanced MM patients.

**Methods:** We performed PPI in 59 patients undergoing advanced MM with Melan-A, tyrosinase, MAGE-2, MAGE-3 and gp-100 peptides based on HLA typing in individuals. The induction of CTLs was assessed by the tetramer or pentamer flow cytometry in 35 patients. Patients showing positive CTL responses to all antigens were defined as complete responder ( $n = 18$ ), and those showing negative responses to at least one applied antigen were classified as incomplete responder ( $n = 17$ ). The primary endpoint of the study was overall survival (OS). For statistical analysis, log-rank test, univariate and multivariate Cox proportional hazard model were used.

**Results:** OS of the complete responders was longer than that of the incomplete responders (median survival time: 55.8 vs 20.3 months, log rank  $P = 0.089$ ). A hazard ratio for the complete responders relative to the incomplete responders was 0.23 (95% confidence interval: 0.06–0.93,  $P = 0.039$ ) in a multivariate Cox proportional hazard model.

**Conclusion:** The induction of CTLs was a novel independent survival factor, and the induction of peptide-specific CTLs by PPI contributes to the prolonged survival and represents an impact on therapeutic approaches in MM.

Unique trial number: UMIN000005706.

© 2014 Japanese Society for Investigative Dermatology. Published by Elsevier Ireland Ltd. All rights reserved.

**Abbreviations:** APC, antigen-presenting cells; CTLs, cytotoxic T lymphocytes; DC, dendritic cells; MM, malignant melanoma; OS, overall survival; PBMCs, peripheral blood mononuclear cells.

\* Corresponding author at: Department of Dermatology, Hamamatsu University School of Medicine, Handayama 1-20-1, Higashi-ku, Hamamatsu 431-3192, Japan. Tel.: +81 53 435 2303; fax: +81 53 435 2368.

E-mail address: [fujiyama@hama-med.ac.jp](mailto:fujiyama@hama-med.ac.jp) (T. Fujiyama).

### 1. Introduction

Malignant melanoma (MM) represents an aggressive skin neoplasm and shows rapid tumor progression and metastasis, leading to a reduced patient survival. Metastatic cutaneous MM is often resistant to conventional therapies, such as chemotherapy, radiation, and surgical resection. On the other hand, MM has a highly immunogenic property, as represented by spontaneous regression occasionally seen in primary tumors [1]. Therefore,

immunotherapy was initially applied to MM, and there have been a considerable number of clinical studies on the immunological treatment modalities for MM [2–4]. Effective presentation of the defined tumor antigens is one of the key factors to develop a durable immunotherapy for advanced MM. Furthermore, the antigen recognition and subsequent antigen-mediated cytotoxicity by T cells infiltrating in tumor microenvironment are essential for efficient promotion of tumor elimination. Clinically, it remains to be elucidated whether the occurrence of antigen-specific T cell responses can be an indicator for prolongation of the patients' survival.

Depletion of T cell-mediated immune responses results in a rapid tumor growth in experimental animal models [5]. Cytotoxic CD8<sup>+</sup> T lymphocytes (CTLs) recognize tumor-associated antigens [6–8]. Adoptive transfer of tumor-specific CTLs is capable of eradicating certain types of tumors [9,10], suggesting that CTLs are crucial for tumor-specific adaptive immunity. CTLs attack tumor cells expressing tumor-associated antigenic peptides with major histocompatibility complex (MHC) class I on the cell surface. When CD8<sup>+</sup> T cells recognize the tumor-specific antigen, they produce interferon- $\gamma$  (IFN- $\gamma$ ) and mediate cytostasis and cell death. Furthermore, CD8<sup>+</sup> T cells promote cell cycle inhibition, apoptosis and angiostasis, and induce the tumoricidal activity of macrophages in tumor microenvironment [11,12].

Antigen-presenting dendritic cells (DCs) play an important role in mediating antigen-specific T-cell responses [9]. Immunotherapies have been improved with the knowledge that T cell antitumor activity can be enhanced with antibodies against immunoregulatory molecules (checkpoint blockade). Current immunotherapy strategies include monoclonal antibodies against tumor cells or immunoregulatory molecules, cell-based therapies such as adoptive transfer of *ex vivo*-activated T cells and natural killer cells, and cancer vaccines. It is an issue how the current understanding of DC and T cell biology might enable the development of next-generation cancer vaccine therapies [13]. Emerging evidence has shown that DC-based vaccination may be potent, while the corresponding method requires a particular technique. Thus, a simple and efficacious procedure is desired for the efficient antigen vaccination and presentation.

We have previously established the simple method by attaching peptide vaccines on the barrier-disrupted skin so that MM-specific CTLs can be induced in a mouse model and a small number of patients [14,15]. This study shows the advantage of novel percutaneous peptide immunization (PPI) for advanced melanoma patients. Based on this finding, we subjected the simple technique to 59 advanced MM patients in multi-institutional joint research. We identified, for the first time, that the induction of CTLs reveals an independent prognostic factor for MM patients.

## 2. Materials and methods

### 2.1. Eligibility and study design

Patients were eligible those who were histologically confirmed as MM, aged 20 years or older, compatible with HLA-A0201 or HLA-A2402. Patients were ineligible with the history of previous chemotherapy, vaccination within 4 weeks, or macroscopic metastatic lesions in the liver or brain. The other ineligible factors included present pregnancy, immunosuppressant administration, and coexistence of eczematous lesions, hepatitis or collagen diseases. All patients provided a written informed consent. The present study was approved by the ethics committee of Hamamatsu University School of Medicine. The study design was an open labeled, single arm, prospective and interventional trial.

### 2.2. Synthetic peptides

Four custom-synthesized peptides including tyrosinase (AFLPWHLRF), MAGE-2 (EYLQLVFGI), MAGE-3 (IMPKAGLLI) and gp-100 (VWKTWGQYW; all from Peptide Institute, Inc., Osaka, Japan) were used as HLA-A2402-restricted epitopes. Modified Melan-A immunodominant cells (ELAGIGLTV; Peptide Institute) were used as HLA-A0201-restricted epitopes [16]. Respective purity was >95% as confirmed by high-pressure liquid chromatography.

### 2.3. Epidermal barrier disruption

To remove *stratum corneum*, 5 cm  $\times$  5 cm square plastic plates were evenly painted with 100 mg/plate of cyanoacrylate (Aron alpha A Sankyo, Tokyo, Japan) or PPT3 tape (LINTEC, Tokyo, Japan), which were attached to the skin for 3 min and removed gently. This procedure was repeated three times at a single spot.

### 2.4. Percutaneous peptide immunization (PPI)

Respective solution of immunization peptides was made prior to topical application. HLA-A0201 subjects received 3 mg of Melan-A peptide in 3 ml of 5% DMSO in phosphate buffered saline (PBS). A cocktail of 3 mg each of tyrosinase, MAGE-2, MAGE-3, and gp-100 peptide in 3 ml of 5% DMSO in PBS was used for HLA-A2402 subjects. In patients who had both HLA-A0201 and HLA-A2402, we used 3 mg of all peptides in 3 ml of 5% DMSO in PBS. Right after the removal of *stratum corneum* (Fig. 1A, top, middle), respective peptide solution was soaked up by the gauze pads (each 5 cm  $\times$  5 cm), which were then applied to each of six barrier-disrupted areas (total area 150 cm<sup>2</sup>) and immediately covered with a dressing film (Fig. 1A, bottom). The pads were removed 24 h later. We avoided the area close to the lymph nodes surgically resected. PPI was repeated ten times at monthly intervals by placing the patches at different areas of the skin. Stable and responding patients were followed up, and when the frequencies of all CTLs became lower than 50% of their maximum points, the patients were eligible for the second cycle of vaccination.

### 2.5. Measurement of immune responses by flow cytometry

Peripheral blood was collected from the patients just before and 3–6 months after the PPI. Peripheral blood mononuclear cells (PBMCs) were purified by standard Ficoll density centrifugation and subjected to flow cytometric analysis. Blood samples were run on a FACS Calibur flow cytometer (BD Bioscience, San Jose, CA) using Cell Quest Software. Phycoerythrin (PE)-labeled MHC pentamers specific for tyrosinase, MAGE-2 and MAGE-3, were custom-synthesized by ProImmune Limited (Littlemore, UK). PE-labeled tetramer for Melan-A was purchased from Beckman Coulter (Villepinte, France). PE-labeled tetramers specific for HIV gag (SLYNTVATL) for HLA-A0201 and tetramers specific for Cytomegalovirus pp65 (QYDPVAALF) or tetramers specific for Epstein-Barr virus BMLF-1 (DYNFVKQLF) for HLA-A2402 were used as controls. PBMCs were stained with PE-labeled HLA-A0201 tetramers or PE-labeled HLA-A2402 pentamers and T-Select Antibodies Gating Kit according to the manufacturer's direction (Medical & Biological Laboratories Co.) including FITC-labeled anti-CD8, PC5-labeled anti-CD4, anti-CD19, and anti-CD13 monoclonal antibodies (mAbs). We analyzed  $1.0 \times 10^5$  PBMCs for CTLs specific to each antigen. Because no HLA-A2402 pentamer or tetramer for gp-100 was available, patients with HLA-A2402 were evaluated with for only tyrosinase, MAGE-2 and MAGE-3-specific CTLs. The frequencies of antigen-specific CTLs from HLA-matched healthy donors were used as control ( $n = 6$  for both types of HLA).

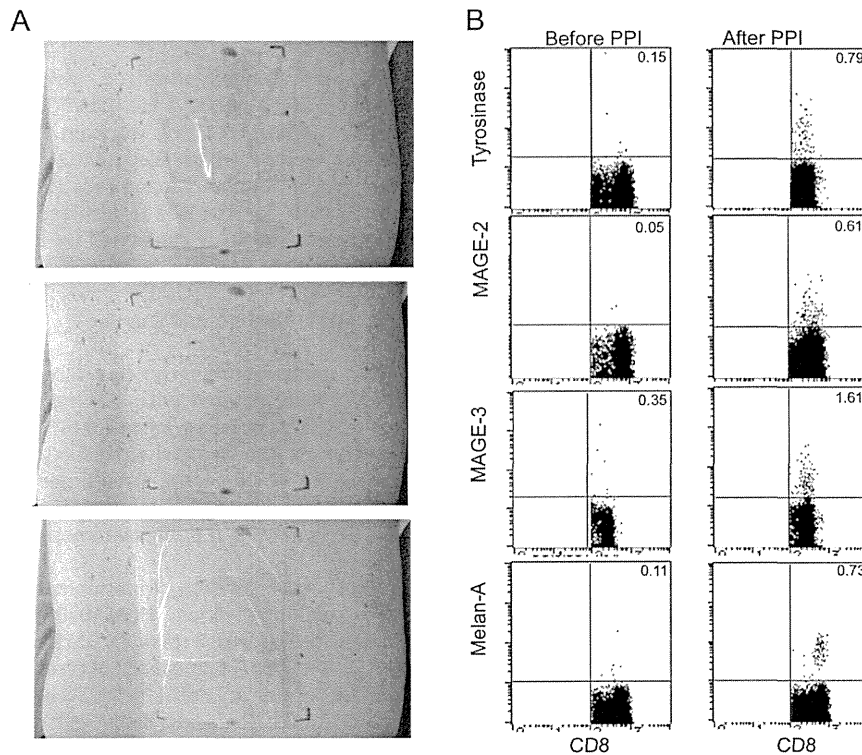


**Fig. 1.** Demonstration of PPI and representative data of flowcytometric analysis of tetramer/pentamer-positive CD8 cells. (A) To remove the *stratum corneum*, PPT3 tape is attached to the skin for 3 min (top) and removed gently (middle). This procedure was repeated three times. The treated skin becomes slightly reddish. Then, the peptide-containing pad is topically applied and covered with a film (bottom). The exposure of the peptides to the skin is performed for 24 h. (B) CD8<sup>+</sup> cells are on the x-axis and tetramer/pentamer-positive cells are on the y-axis.

## 2.6. CTL response evaluation

When the frequency of the antigen-specific CTLs was equal or greater than mean + 2SD of the control, we considered the value as positive. When it was lower than mean + 2SD of the control, it was considered negative. Patients showing positive responses to all applied antigens were defined as complete responder, and those showing negative responses to at least one applied antigen were classified as incomplete responder. Therefore, the incomplete responder also included the complete non-responder.

## 2.7. Clinical response evaluation

Tumor evaluation included physical examination and axial computed tomography (CT) scans before treatment. Stable and responding patients were evaluated every 6 months by physical examination, blood tests and CT scan. Overall response was evaluated by modification of Response Evaluation Criteria in Solid Tumors (RECIST 1.1).

## 2.8. Statistical analysis

The analysis aimed at determining whether high responders to PPI have a better prognosis than do the low or non-responders. The primary endpoint of the study was overall survival (OS), which was defined as the interval between the date of PPI initiation and the date of death or last follow-up. The survival curve was calculated by Kaplan–Meier product limit method. The association between OS and prognostic factors were assessed by HR and 95% CI used multivariate Cox proportional hazard model using Landmark method [17]. As the study did not employ randomization because of the properties of the study, we defined multivariate analysis adjusted for established prognostic factors as a primary analysis.

Potential confounding factors considered in the multivariate analysis were age as a continuous variable, sex (male or female), primary site (limbs, mucosa, or others), LDH (<400 IU/L or  $\geq$ 400 IU/L), PS (0, 1, or 2–4), history of chemotherapy (never or ever), and disease stage (I–III or IV). For reference, univariate analysis was done by the log-rank test and univariate Cox proportional hazard models. Statistical analyses were performed using STATA version 10 (Stata Corporation, College Station, TX). The frequencies of specific CTLs were compared by Wilcoxon *T* test. We defined a priori *P*-value less than 0.05 in a primary analysis as threshold to indicate significant impact of induction of CTLs by PPI. For other analyses, we conventionally applied *P*-value less than 0.05 as statistically significant.

## 3. Results

In April 2003 to March 2011, 59 patients with advanced MM were subjected to PPI by using the *stratum corneum*-removal tape-stripping technique (Fig. 1A). No hematologic abnormality was observed after PPI. The most frequent adverse events were generalized progressive vitiligo (12 out of 59 patients) after several months of immunization. Four patients had irritant dermatitis at the treated sites.

CTLs were evaluated in 35 patients before and after PPI, and 24 patients were excluded in the following analysis, because CTLs were not examined either pre- or post-PPI or both. Among the 35 patients, 27 and 15 patients were positive for HLA-A2402 and A0201, respectively. Seven patients were positive for both HLA types. As represented by a patient responding well to PPI (Fig. 1B), the dot-plot flow cytometry revealed the frequencies of CD8<sup>+</sup> CTLs specific to tyrosinase, MAGE-2, MAGE-3, and Melan-A were all increased after 3 to 6-time PPI treatments as compared to the pre-PPI values.

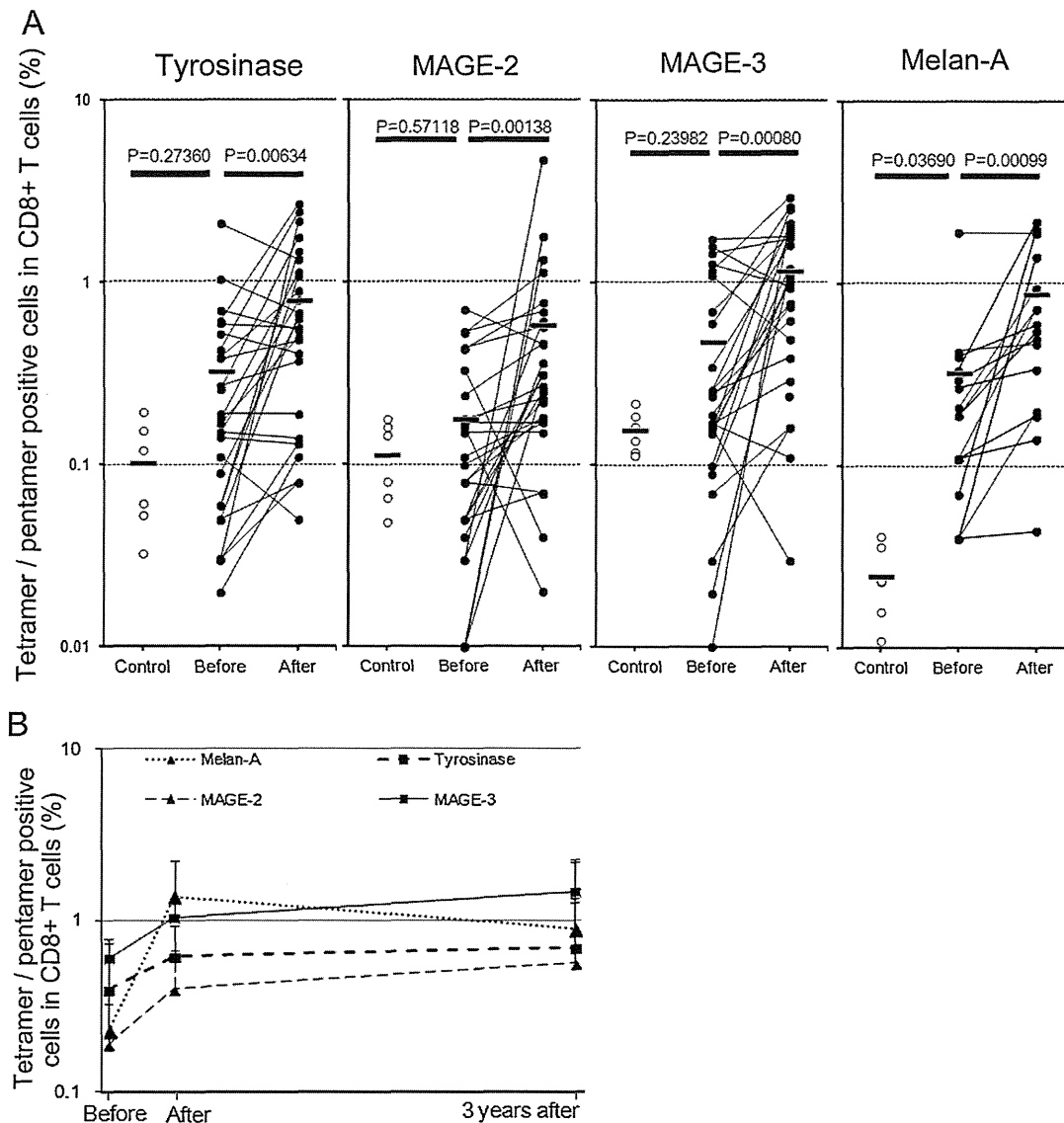


**Fig. 2.** Percentage of each tetramer/pentamer-positive cells in CD8<sup>+</sup> T cells. (A) The frequencies of CD8<sup>+</sup> CTLs specific to tyrosinase, MAGE-2, MAGE-3, and Melan-A were monitored before and after 3 to 6-time PPI treatments. The control represents the data from healthy subjects. (B) Three-year follow up of the frequencies of the applied antigen-specific CTLs ( $n = 3$  for Melan-A,  $n = 6$  for tyrosinase, MAGE-2 and MAGE-3).

Even before PPI treatment, the frequencies of peptide-specific CTLs in MM patients were largely higher than those of the healthy control subjects. The pre-therapy CTL frequencies to Melan-A were significantly higher, and those to the other three antigens tended to be higher than the controls (Fig. 2A). More importantly, the CTL frequencies further increased significantly after PPI. The  $P$ -values for tyrosinase-, MAGE-2-, MAGE-3- and Melan-A-specific CTLs were 0.006, 0.001, 0.001 and 0.001, respectively (Wilcoxon  $t$ -test). We examined the degree of patients' responsiveness to PPI by monitoring the CTL frequencies. Among the patients with HLA A2402, 19 of 27, 19 of 27 and 23 of 27 patients developed positive responses to tyrosinase, MAGE-2 and MAGE-3, respectively (Fig. 2A). We monitored the frequencies of CTL for 3 years in several complete responders. The frequencies of the antigen-specific CTL remained or slightly increased in the patients who survived and showed positive responses to tyrosinase, MAGE-2, and MAGE-3 (Fig. 2B), presumably by the repeated course of immunization. In addition, among the patients with HLA A0201, 12 of 15 patients developed positive responses to Melan-A. Eighteen

patients showed positive responses to all applied peptide antigens, and we defined them as complete responders. The rest of the patients ( $n = 17$ ) were negative for at least one applied antigen, and we defined them as incomplete responders. Among the incomplete responders, 2 patients were negative to all applied antigens. There was no significant difference in the patients' characteristics between the complete and incomplete responders (Table 1).

The overall survival time in the complete and incomplete responders were investigated by Kaplan–Meier method (Fig. 3). At a median follow-up time of 16.2 months, the complete responder group had a longer survival than the incomplete responder group (MST; 55.8 vs 20.3 months,  $P = 0.089$ ). Univariate and multivariate analyses were performed to examine the relationship between OS and CTL induction (Table 2). The multivariate analysis was adjusted for age, sex, primary site, LDH, PS, history of chemotherapy, and disease stage. The complete responder group had a significantly higher survival than did the incomplete responder group (HR = 0.23, 95% CI: 0.06–0.93,  $P = 0.039$ ). This association was consistently observed when we exclude primary site from the

**Table 1**  
Patient characteristics.

	CTL induction		P
	Complete responder	Incomplete-responder	
Age (mean, SD)	54.9 ± 16.9	57.3 ± 18.1	0.687
Sex			0.631
Male	12	10	
Female	6	7	
Primary site			0.128
Limb	9	5	
Mucosa	0	3	
Other	9	9	
LDH			0.714
<400 IU/L	15	14	
≥400 IU/L	1	2	
PS			0.803
0, 1	16	14	
≥2	1	2	
History of chemotherapy			0.113
Never	2	6	
Ever	16	10	
Disease stage			0.369
I–III	3	5	
IV	15	12	

model (data not shown). Univariate analysis showed consistent association between OS and CTL response after PPI. Since we used a cocktail of the peptides, we were unable to directly compare the efficacy of each peptide. Among the incomplete responders, however, we observed no significant correlation between the overall survival and the antigen incapable of inducing positive responses. Moreover, there was no significant difference in the overall survival between HLA-A0201 and A2402 (log-rank  $P = 0.213$ ), suggesting that there was no priority in the efficacy of A0201 or A2402-related peptides.

#### 4. Discussion

It was reported that the objective response (PR + CR) in the DC vaccination therapies with peptides was 7.8% [18]. In the present study, at least 3-month period was required for the induction of CTLs. Since 50 of 59 patients showed PD, we were able to monitor the frequencies of CTLs after PPI in only 35 patients. Nevertheless, we showed that the superior survival of advanced MM patients significantly correlated with the complete induction of peptide-specific CTLs by PPI. Multivariate analyses further revealed that the complete responder is an independent survival factor in the MM patients who received PPI. Thus, the vaccination has a clinical impact on therapeutic approaches in metastatic MM. Even before the PPI treatment, the frequencies of specific CTLs in the blood were higher than the controls, and they further increased after the treatment, suggesting the contribution of CTLs to the therapeutic

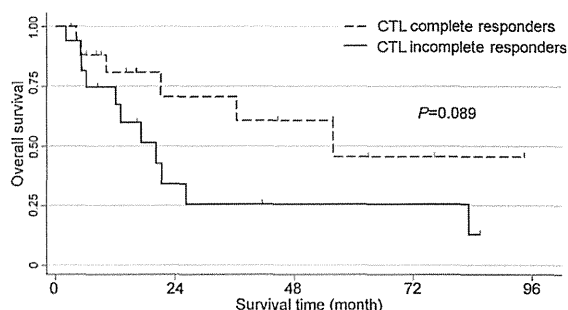


**Fig. 3.** Overall survival time in association with CTL induction. Patients showing positive responses to all four antigens were defined as complete responder, and those showing negative responses to at least one applied antigen were classified as incomplete responder. The complete responders show a superior survival as compared with the incomplete responders by Kaplan–Meier method.

effect. We have previously shown that peptide-specific CTLs are successfully induced by PPI and infiltrate in the tumor lesions, and can reduce the tumor size [14]. In agreement with our finding, it was reported that the presence of tumor-infiltrating lymphocytes in the primary sites or in the metastatic foci of lymph nodes is an independent prognostic factor for cutaneous MM [19,20]. Since Melan A and tyrosinase are expressed not only in melanoma cells but also by normal melanocytes, autoimmune reactions possibly occur against normal melanocytes, as the development of ocular and systemic autoimmunity following the immunotherapy has been documented. All of our patients were screened for uveitis before and after the PPI and none showed positive findings. The common adverse events were systemic progressive vitiligo, seen in 12 patients, but no life threatening side effect was observed.

On the other hand, recent studies have suggested that MM is resistant to the CD8<sup>+</sup> T cell-based vaccination therapy. A number of mechanisms have been put forward to explain the resistance [21]. The tumor induces peripheral tolerance of tumor-specific CD8<sup>+</sup> T cells by their clonal deletion [22] or peripheral anergy [23,24], or induction of regulatory T cells [25]. The tumor cell *per se* develops immune evasion mechanisms to prevent recognition and killing by CTLs [26]. More recently, promotion of PD-1/PD-L1 engagement [27] and suppression of Th17-derived cytokines [28] have been shown to down-modulate the CTL-mediated melanoma immunity. The MM-specific CD8<sup>+</sup> T cell was detected in peripheral blood of 68% of advanced stage MM patients, but the induction of these cells was not accompanied by clinically significant antitumor effect [29]. For efficacious control of the disease, antigen-specific CTLs should be functionally active, capable of homing to the tumor sites, and resistant to the tumor microenvironment.

We used cutaneous DCs as APCs. Recently, the classical paradigm for LCs has been revised. LCs migrate to draining lymph nodes and initiate T cell priming. However, LCs may not be indispensable for contact hypersensitivity, but even serve as a

**Table 2**  
The association between CTL induction and overall survival.

		Univariate analysis			Multivariate analysis		
		HR	95% CI	P	HR	95% CI	P
CTL induction	Incomplete vs complete	0.43	(0.16–1.17)	0.098	0.23	(0.06–0.93)	0.039
Age		0.97	(0.94–1.00)	0.076	0.97	(0.92–1.01)	0.141
Sex	Male vs female	1.01	(0.37–2.76)	0.979	0.83	(0.18–3.90)	0.815
Primary site	Limb	1.00	Ref.		1.00	Ref.	
	Mucosa	1.02	(0.20–5.11)	0.985	0.37	(0.06–2.47)	0.306
	Other	1.61	(0.57–4.59)	0.373	0.46	(0.05–3.86)	0.472
LDH	<400 vs ≥400 IU/L	3.14	(0.68–14.50)	0.143	1.05	(0.10–10.96)	0.969
PS	0, 1 vs 2–4	19.91	(1.11–358.25)	0.042	25.31	(0.85–756.82)	0.062
Chemotherapy	Never vs ever	0.86	(0.27–2.72)	0.803	0.53	(0.09–3.04)	0.476
Disease stage	I–III vs IV	1.50	(0.49–4.66)	0.479	3.32	(0.62–17.78)	0.162

regulator for the sensitivity in mice [30,31]. In the tumor immunity, however, the depletion of LCs at the time of skin immunization dramatically reduced the tumor-protective effect [32], suggesting the importance of LCs for percutaneous immunization. LCs can clearly fulfill an immunogenic role during vaccination against cancer *in vivo* [33]. Although the role of LCs in the induction of skin immune responses remains to be constitutively demonstrated, immunization strategies of antigen application to the skin have been proven to be feasible and to elicit systemic immunity [34,35]. Accordingly, several challenges for the induction of anti-tumor immune responses using LCs or cutaneous DCs have been reported [9,14,32,36].

To our knowledge, this is the first report demonstrating the effective induction of the tumor specific CTLs in MM patients who received PPI treatment. Our study suggests that PPI is simple and safe and relatively effective treatment for MM, and thus, it can be one of the therapeutic options. To improve the response rate and overall survival, selection of antigenic peptides, addition of helper epitope peptides, and usage of adjuvants should be considered in future.

#### Acknowledgment

This study was supported by Grants-in-Aid for Scientific Research from the Ministry of Health, Labour, and Welfare in Japan.

#### References

- [1] Morton DL, Wanek L, Nizze JA, Elashoff RM, Wong JH. Improved long-term survival after lymphadenectomy of melanoma metastatic to regional nodes. Analysis of prognostic factors in 1134 patients from the John Wayne Cancer Clinic. *Ann Surg* 1991;214: 491–9, discussion 499–501.
- [2] Fang L, Lonsdorf AS, Hwang ST. Immunotherapy for advanced melanoma. *J Invest Dermatol* 2008;128:2596–605.
- [3] Tuting T. T cell immunotherapy for melanoma from bedside to bench to barn and back: how conceptual advances in experimental mouse models can be translated into clinical benefit for patients. *Pigment Cell Melanoma Res* 2013;26:441–56.
- [4] Topalian SL, Weiner GJ, Pardoll DM. Cancer immunotherapy comes of age. *J Clin Oncol* 2011;29:4828–36.
- [5] Koebel CM, Vermi W, Swann JB, Zerafa N, Rodig SJ, Old LJ, et al. Adaptive immunity maintains occult cancer in an equilibrium state. *Nature* 2007;450:903–7.
- [6] Ikeda H, Ohta N, Furukawa K, Miyazaki H, Wang L, Kuribayashi K, et al. Mutated mitogen-activated protein kinase: a tumor rejection antigen of mouse sarcoma. *Proc Natl Acad Sci U S A* 1997;94:6375–9.
- [7] van der Bruggen P, Traversari C, Chomez P, Lurquin C, De Plaen E, Van den Eynde B, et al. A gene encoding an antigen recognized by cytolytic T lymphocytes on a human melanoma. *Science* 1991;254:1643–7.
- [8] Wolfel T, Hauer M, Schneider J, Serrano M, Wolfel C, Klehmann-Hieb E, et al. A p16INK4a-insensitive CDK4 mutant targeted by cytolytic T lymphocytes in a human melanoma. *Science* 1995;269:1281–4.
- [9] Grabbe S, Beissert S, Schwarz T, Granstein RD. Dendritic cells as initiators of tumor immune responses: a possible strategy for tumor immunotherapy? *Immunol Today* 1995;16:117–21.
- [10] Banchereau J, Steinman RM. Dendritic cells and the control of immunity. *Nature* 1998;392:245–52.
- [11] Smyth MJ, Dunn GP, Schreiber RD. Cancer immunosurveillance and immunoeediting: the roles of immunity in suppressing tumor development and shaping tumor immunogenicity. *Adv Immunol* 2006;90:1–50.
- [12] Dunn GP, Old LJ, Schreiber RD. The three Es of cancer immunoeediting. *Annu Rev Immunol* 2004;22:329–60.
- [13] Palucka K, Banchereau J. Dendritic-cell-based therapeutic cancer vaccines. *Immunity* 2013;39:38–48.
- [14] Yagi H, Hashizume H, Horibe T, Yoshinari Y, Hata M, Ohshima A, et al. Induction of therapeutically relevant cytotoxic T lymphocytes in humans by percutaneous peptide immunization. *Cancer Res* 2006;66:10136–44.
- [15] Seo N, Tokura Y, Nishijima T, Hashizume H, Furukawa F, Takigawa M. Percutaneous peptide immunization via corneum barrier-disrupted murine skin for experimental tumor immunoprophylaxis. *Proc Natl Acad Sci U S A* 2000;97:371–6.
- [16] Sliz P, Michielin O, Cerottini JC, Luescher I, Romero P, Karplus M, et al. Crystal structures of two closely related but antigenically distinct HLA-A2/melanocyte-melanoma tumor-antigen peptide complexes. *J Immunol* 2001;167:3276–84.
- [17] Anderson JR, Cain KC, Gelber RD. Analysis of survival by tumor response. *J Clin Oncol* 1983;1:710–9.
- [18] Nakai N, Hartmann G, Kishimoto S, Katoh N. Dendritic cell vaccination in human melanoma: relationships between clinical effects and vaccine parameters. *Pigment Cell Melanoma Res* 2010;23:607–19.
- [19] Clemente CG, Mihm Jr MC, Bufalino R, Zurrida S, Collini P, Cascinelli N. Prognostic value of tumor infiltrating lymphocytes in the vertical growth phase of primary cutaneous melanoma. *Cancer* 1996;77:1303–10.
- [20] Mihm Jr MC, Clemente CG, Cascinelli N. Tumor infiltrating lymphocytes in lymph node melanoma metastases: a histopathologic prognostic indicator and an expression of local immune response. *Lab Invest* 1996;74:43–7.
- [21] Huang Y, Shah S, Qiao L. Tumor resistance to CD8+ T cell-based therapeutic vaccination. *Arch Immunol Ther Exp (Warsz)* 2007;55:205–17.
- [22] Aichele P, Brduscha-Riem K, Zinkernagel RM, Hengartner H, Pircher H. T cell priming versus T cell tolerance induced by synthetic peptides. *J Exp Med* 1995;182:261–6.
- [23] Van Parijs L, Abbas AK. Homeostasis and self-tolerance in the immune system: turning lymphocytes off. *Science* 1998;280:243–8.
- [24] Shevach EM. CD4+ CD25+ suppressor T cells: more questions than answers. *Nat Rev Immunol* 2002;2:389–400.
- [25] Seo N, Hayakawa S, Takigawa M, Tokura Y. Interleukin-10 expressed at early tumour sites induces subsequent generation of CD4(+) T-regulatory cells and systemic collapse of antitumour immunity. *Immunology* 2001;103:449–57.
- [26] Lee HM, Timme TL, Thompson TC. Resistance to lysis by cytotoxic T cells: a dominant effect in metastatic mouse prostate cancer cells. *Cancer Res* 2000;60:1927–33.
- [27] Hino R, Kabashima K, Kato Y, Yagi H, Nakamura M, Honjo T, et al. Tumor cell expression of programmed cell death-1 ligand 1 is a prognostic factor for malignant melanoma. *Cancer* 2010;116:1757–66.
- [28] Hayata K, Iwahashi M, Ojima T, Katsuda M, Iida T, Nakamori M, et al. Inhibition of IL-17A in tumor microenvironment augments cytotoxicity of tumor-infiltrating lymphocytes in tumor-bearing mice. *PLoS One* 2013;8:e53131.
- [29] van Oijen M, Bins A, Elias S, Sein J, Weder P, de Gast G, et al. On the role of melanoma-specific CD8+ T-cell immunity in disease progression of advanced-stage melanoma patients. *Clin Cancer Res* 2004;10:4754–60.
- [30] Kaplan DH, Jenison MC, Saeland S, Shlomchik WD, Shlomchik MJ. Epidermal langerhans cell-deficient mice develop enhanced contact hypersensitivity. *Immunity* 2005;23:611–20.
- [31] Kissenpfennig A, Henri S, Dubois B, Laplace-Builhe C, Perrin P, Romani N, et al. Dynamics and function of Langerhans cells *in vivo*: dermal dendritic cells colonize lymph node areas distinct from slower migrating Langerhans cells. *Immunity* 2005;22:643–54.
- [32] Stoitzner P, Green LK, Jung JY, Price KM, Tripp CH, Malissen B, et al. Tumor immunotherapy by epicutaneous immunization requires langerhans cells. *J Immunol* 2008;180:1991–8.
- [33] Romani N, Clausen BE, Stoitzner P. Langerhans cells and more: langerin-expressing dendritic cell subsets in the skin. *Immunol Rev* 2010;234:120–41.
- [34] Warger T, Schild H, Rechtsteiner G. Initiation of adaptive immune responses by transcutaneous immunization. *Immunol Lett* 2007;109:13–20.
- [35] Partidos CD, Beignon AS, Semetey V, Briand JP, Muller S. The bare skin and the nose as non-invasive routes for administering peptide vaccines. *Vaccine* 2001;19:2708–15.
- [36] Eisenberg G, Machlenkin A, Frankenburg S, Mansura A, Pitcovski J, Yefenof E, et al. Transcutaneous immunization with hydrophilic recombinant gp100 protein induces antigen-specific cellular immune response. *Cell Immunol* 2010;266:98–103.



ORIGINAL ARTICLE

## Measurement of cutaneous lymphatic flow rates in patients with skin cancer: area extraction method

Masao FUJIWARA,<sup>1</sup> Michifumi SAWADA,<sup>2</sup> Akira KASUYA,<sup>3</sup> Yuki MATSUSHITA,<sup>1</sup> Moe YAMADA,<sup>1</sup> Hidekazu FUKAMIZU,<sup>1</sup> Yasuhiro MAGATA,<sup>4</sup> Yoshiki TOKURA,<sup>3</sup> Harumi SAKAHARA<sup>2</sup>

<sup>1</sup>Departments of Plastic and Reconstructive Surgery, <sup>2</sup>Radiology, <sup>3</sup>Dermatology, and <sup>4</sup>Department of Molecular Imaging, Medical Photonics Research Center, Hamamatsu University School of Medicine, Hamamatsu, Japan

### ABSTRACT

Some recent reports have revealed that the long scintigraphic appearance time (SAT), defined as the time between radionuclide injection and first sentinel lymph node (SLN) visualization in lymphoscintigraphy, is a negative predictive parameter of nodal metastasis in patients with melanoma. However, most of the methods used to measure the SAT were ambiguous because they utilized visualization in lymphoscintigraphy. We herein introduce a novel method by which to measure the SAT and lymphatic flow rate. The data of 33 patients with primary skin cancer were used. Sequential images were obtained using dynamic lymphoscintigraphy, and a time–activity curve of the SLN was created. The time at which the counts reached plateau was newly defined as an alternative to the SAT and was termed the scintigraphic saturation time (SST). The figure obtained by division of the distance by the SST was newly defined as an alternative to the lymphatic flow rate and termed the lymphatic transit rate (LTR). The SST was clearly determined. It ranged from 220 to 1430 s (mean, 805 s). Pathological examination revealed nodal metastasis in five patients. In 28 patients without metastasis, the mean LTR was in the order of lower limbs ( $4.07 \pm 0.35$  cm/min), upper limbs ( $2.67 \pm 0.33$  cm/min), trunk ( $1.79 \pm 0.47$  cm/min), and head and neck ( $1.11 \pm 0.22$  cm/min). The LTRs were higher in patients with nodal metastasis than those without. This method may be effective for accurate measurement of the SAT and lymphatic flow rate.

**Key words:** <sup>99m</sup>Tc-phytate, lymphatic flow rate, lymphoscintigraphy, scintigraphic appearance time, skin cancer.

### INTRODUCTION

In patients with skin cancer, the lymphatic flow rate has been measured previously with lymphoscintigraphy to determine the time required to reach the regional lymph nodes from the injection sites around the tumor, and thus ensure successful sentinel lymph node (SLN) biopsy.<sup>1–3</sup>

Recently, in animal melanoma models, an association between an increased lymphatic flow rate and higher rates of metastasis was reported.<sup>4–6</sup> In addition, some reports revealed that a long scintigraphic appearance time (SAT), which is conventionally defined as the time between radionuclide injection and first SLN visualization in lymphoscintigraphy, is a negative predictive parameter for nodal metastasis in patients with melanoma.<sup>7–9</sup> Therefore, the relationship between lymph node metastasis and the time required to reach the SLN from the tumor site has become an issue of renewed interest.<sup>7–11</sup>

However, the methods used to measure the lymphatic flow rate in previous reports vary.<sup>1–3,7–11</sup> Most of the methods used

to measure the SAT and lymphatic flow rate in previous reports were ambiguous because the time was determined by visualization in lymphoscintigraphy.<sup>1,7–10</sup>

A more accurate methodology with which to measure the SAT and lymphatic flow rate is therefore required. This report aims to introduce a novel method by which to measure the SAT and lymphatic flow rate of various parts of the human body using a time–activity curve of dynamic lymphoscintigraphy.

### PATIENTS AND METHODS

The data of 33 patients with histologically proven primary skin cancer (15 male and 18 female patients; age range, 21–90 years) were used. All patients (19 with melanoma, 10 with squamous cell carcinoma, one with invasive extramammary Paget's disease, one with apocrine adenocarcinoma, one with Merkel cell carcinoma, and one with eccrine porocarcinoma) underwent lymphoscintigraphy. Two SLNs were

Correspondence: Masao Fujiwara, M.D., D.D.S., Ph.D., Department of Plastic and Reconstructive Surgery, Hamamatsu University School of Medicine, 1–20-1 Handayama, Hamamatsu, Shizuoka 431-3192, Japan. Email: masafuj@nth.biglobe.ne.jp

Received 12 February 2014; accepted 2 April 2014.

detected in three patients, and the remaining patients each had one SLN. The initial locations of skin cancer were the head and neck in five patients (15%), trunk in 11 patients (33%), upper limb in six patients (18%), and lower limb in 11 patients (33%). Pathological examination revealed nodal metastasis in five patients (15%). The study was approved by the institutional review board and conducted in accordance with the Declaration of Helsinki. Informed consent was obtained from each patient.

### Area extraction method

Dynamic lymphoscintigraphy was performed using  $^{99m}\text{Tc}$ -phytate (Techne Phytate Kit; Fujifilm RI Pharma, Tokyo, Japan) with 0.1-mL intracutaneous injections into six points ( $6 \times 18.5 \text{ MBq } ^{99m}\text{Tc}$ -phytate) around the primary tumor or excisional biopsy wound. Image acquisition started simultaneously with the first injection using a gamma camera (Millennium VG Hawkeye option; GE Healthcare, Wauwatosa, WI).

As defined by Uren *et al.*,<sup>12</sup> we considered an SLN to be any lymph node that receives lymphatic drainage directly from a tumor site. The patient remained supine for imaging of the SLN. Dynamic images including both the SLN and the vicinity of the SLN were obtained every 10 s for a period of 30 min, and time-activity curves of the SLN were created in the following manner. A region of interest (ROI) encompassing the SLN was drawn in each dynamic image, and tracer counts were calculated from these ROIs with a built-in function of Xeleris Workstation (GE Healthcare). The counts per second of the region were plotted against time. The time at which the counts reached plateau was newly defined as an alternative to the SAT of the SLN, and the time was termed the scintigraphic saturation time (SST) (Fig. 1). The data of six dynamic image frames were summed, and dynamic lymphoscintigraphic scans were obtained every 60 s (Fig. 2). In addition, 1- and 2-h postinjection delayed images were obtained. The distance between the primary focus and the SLN was measured along the line delineated by real-time fluorescence navigation with indocyanine green, as we previously reported.<sup>13</sup> The figure obtained by dividing the distance by the SST was newly defined as an alternative to the lymphatic flow rate and termed the lymphatic transit rate (LTR) ( $\text{LTR} = \text{distance from the tumor to the SLN/SST}$ ). All data are expressed as mean  $\pm$  standard deviation.

### Lymphatic vessel density

To analyze the peritumoral lymphatic vessel density, data were obtained from five patients without nodal metastasis and five patients with nodal metastasis. Each group of five patients included three patients with a tumor located in the trunk and two with a tumor located in a lower limb.

For immunohistochemistry, serial sections of paraffin-embedded skin tumor samples were cut, dewaxed, and rehydrated prior to microwave antigen retrieval (800 W) in Tris/EDTA (Trizma, 100 mmol/L; EDTA, 2 mmol/L) at a pH of 9 for 8 min. Endogenous peroxidase activity was blocked by incubation for 5 min in 3% hydrogen peroxidase followed by two phosphate-buffered saline (PBS) washes (NaCl, 137.00 mmol/

L; KCl, 2.68 mmol/L;  $\text{Na}_2\text{HPO}_4$ , 10.00 mmol/L;  $\text{KH}_2\text{PO}_4$ , 1.76 mmol/L). Nonspecific binding was prevented by incubation in normal serum for 20 min in a humid chamber (for D2-40 [1:1, mouse monoclonal; Nichirei, Tokyo, Japan], 5% human serum  $\text{wv}^{-1}$  in PBS). The slides were incubated in antibodies to D2-40 overnight at 4°C. The slides were washed twice (PBS/Tween, 0.05%  $\text{vv}^{-1}$ ), and the nonimmune block was repeated. Secondary antibody (Simple Stain PO; Nichirei, Tokyo, Japan) was used. The captured images from immunohistochemistry by D2-40 were analyzed to measure the numbers of lymphatic ducts. For each section, the fields in the peritumoral area with the highest lymphatic vessel density ("hot spots") were evaluated at  $\times 100$  magnification. Peritumoral lymphatic vessels were defined as D2-40-positive vessels within an area of 100  $\mu\text{m}$  from the tumor border. The unpaired Student's *t*-test was used to determine the statistical significance of sample means.

## RESULTS

The patients' clinical characteristics, including age, sex, body mass index (BMI), tumor location, SST, and LTR, are shown in Tables 1, 2. At a cut-off point of 70 years, a correlation between age and LTR was not demonstrated. A correlation between sex and LTR was not shown. The mean LTRs were lower in patients with a BMI of  $\geq 23$  than in patients with a BMI of  $< 23$  (Table 3).

The SST was more clearly determined using the area extraction method than with the conventional method using visualization (Figs 1, 2). The SST ranged from 220 to 1430 s (mean, 805 s).

In 28 patients without nodal metastasis, the LTR varied according to the location of the skin cancer. The mean LTR was in the order of lower limbs ( $4.07 \pm 0.35 \text{ cm/min}$ ), upper limbs ( $2.67 \pm 0.33 \text{ cm/min}$ ), trunk ( $1.79 \pm 0.47 \text{ cm/min}$ ), and head and neck ( $1.11 \pm 0.22 \text{ cm/min}$ ) (Fig. 3). The LTRs were higher in patients with nodal metastasis than those without. The mean LTR in the trunk was  $3.37 \text{ cm/min}$  (range, 2.57–4.73  $\text{cm/min}$ ) in metastatic SLNs and  $1.79 \text{ cm/min}$  (range, 0.95–2.24  $\text{cm/min}$ ) in histologically normal SLNs. The mean LTR in the lower limb was  $5.31 \text{ cm/min}$  (range, 4.85–5.76  $\text{cm/min}$ ) in metastatic SLNs and  $4.07 \text{ cm/min}$  (range, 3.29–4.33  $\text{cm/min}$ ) in histologically normal SLNs (Tables 1, 2).

The peritumoral lymphatic vessel density was significantly higher in cases with nodal metastasis ( $18.8 \pm 6.3/\text{hpf}$ ) than in cases without metastasis ( $9.2 \pm 3.4/\text{hpf}$ ) ( $P < 0.05$ , unpaired Student's *t*-test) (Fig. 4).

## DISCUSSION

To measure the lymphatic flow rate, Akhras *et al.*<sup>11</sup> measured the removal rate of  $^{99m}\text{Tc}$ -labeled human immunoglobulin G from the vicinity of melanomas using quantitative lymphoscintigraphy. Uren *et al.*<sup>2,3</sup> measured the distance that  $^{99m}\text{Tc}$ -antimony sulfide colloid travelled in 10 min in various body sites following intradermal injection in patients with melanoma. Although the above-mentioned methods are accurate, they are

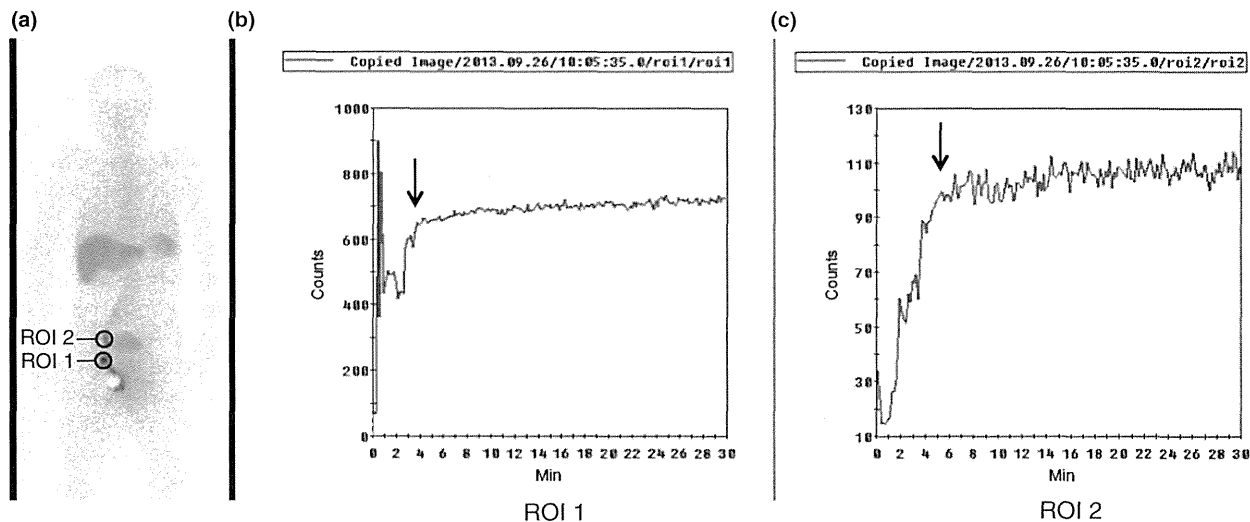


**Figure 1.** Time-activity curve in Case 9. (a) Anterior image. The sentinel lymph node (SLN) was encompassed by a circle of region of interest 1 (ROI1), and a second-tier node was encompassed by a circle of ROI2. (b) Time-activity curve at the SLN. The arrow indicates the scintigraphic saturation time (SST) of the SLN in the right inguinal region. Because a syringe containing radionuclide was near the SLN, the counts of the ROI1 increased in the initial phase. (c) Time-activity curve at the second-tier node. An arrow indicates the SST of the second-tier node in the external iliac region.

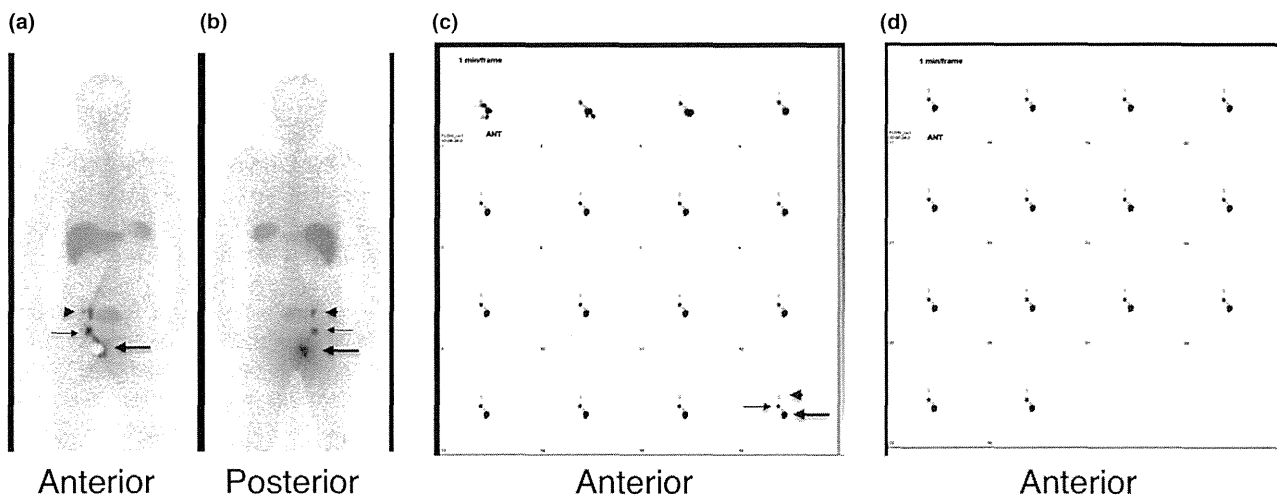


**Figure 2.** Static and dynamic lymphoscintigraphy in Case 9. (a, b) Invasive extramammary Paget's disease of the scrotum (large arrow). Anterior and posterior 60-min delayed images showed the right inguinal sentinel lymph node (SLN) (small arrow) and second-tier node in the right external iliac region (arrowhead). On the anterior view, a primary tumor was shielded by a lead plate. (c) Anterior-view dynamic lymphoscintigraphic scan every 60 s (30 min postinjection). Although tracer counts reached plateau at 220 s postinjection (which corresponded to the scan image 4 min postinjection), it was difficult to determine the time at which the SLN was clearly visually outlined because the SLN initially emerged. Primary tumor (large arrow), SLN (small arrow), second-tier node (arrowhead).

not practical because it is not possible to measure the time taken to travel from lesions to the SLN.

In previous reports, the SAT was determined as the time from the first injection of radionuclide until the SLN was clearly visually outlined in lymphoscintigraphy.<sup>1,7-10</sup> However, Nathan-

son *et al.*<sup>1</sup> mentioned that the lymphatic flow data generated by their method are rough estimates because of limitations inherent in the methodology. Although the distances from the primary tumor sites are accurate, the elapsed time from the injection site is a crude approximation. The time from the first

**Table 1.** Clinical profile of patients without nodal metastasis

Case	Age (years)	Sex	BMI	Tumor	Location	Site of Sentinel lymph node	SST (sec)	Distance (cm)	Lymphatic transit rate (cm/min)
1	65	F	26.41	SCC	Parietal	Rt. deep cervical	1366	22	0.97
						Lt. deep cervical	1430	4	1.01
2	31	F	17.65	SCC	Rt. occipital	Rt. posterior auricular	308	7	1.36
3	73	M	24.60	Melanoma	Nasal root	Lt. submandibular	700	12	1.03
						Rt. submandibular	800	12	0.90
4	90	M	22.16	Melanoma	Rt. pre-auricular	Rt. submandibular	414	8	1.16
5	35	M	19.41	Melanoma	Rt. lateral neck	Rt. submandibular	231	6	1.56
6	35	M	23.55	Melanoma	Lt. anterior chest	Lt. axillary	270	9	2.00
7	55	M	17.90	SCC	Median anterior chest	Rt. axillary	630	19	1.81
						Lt. axillary	521	16	1.84
8	34	M	23.83	AAC	Lt. axilla	Lt. axillary	380	6	0.95
9	65	M	20.31	EMP	Rt. scrotum	Rt. inguinal	220	8	2.18
10	80	F	25.02	Melanoma	Rt. Buttock	Rt. inguinal	964	34	2.24
11	81	F	23.05	Melanoma	Rt. Buttock	Rt. inguinal	636	23	2.17
12	81	F	22.16	Melanoma	Rt. Buttock	Rt. inguinal	1200	39	1.95
13	86	M	27.45	SCC	Rt. Lower abdomen	Rt. Inguinal	818	13	0.95
14	63	M	24.64	SCC	Rt. upper arm	Rt. axillary	320	13	2.44
15	81	F	28.75	SCC	Rt. forearm	Rt. axillary	1050	36	2.06
16	77	M	25.76	SCC	Rt. Palm	Rt. axillary	880	44	3.00
17	69	M	19.28	SCC	Lt. dorsal hand	Lt. axillary	1062	50	2.82
18	83	F	23.27	Melanoma	Rt. thumb	Rt. axillary	940	46	2.94
19	65	F	20.95	SCC	Lt. index finger	Lt. axillary	1040	48	2.77
20	53	F	19.30	Melanoma	Rt. lower leg	Rt. inguinal	550	37	4.03
21	53	F	30.81	Melanoma	Lt. lower leg	Lt. inguinal	583	42	4.32
22	63	F	23.71	Melanoma	Lt. lateral foot	Lt. inguinal	1404	77	3.29
23	83	M	21.97	Melanoma	Lt. sole	Lt. inguinal	1125	79	4.21
24	68	M	17.78	SCC	Lt. sole	Lt. inguinal	1100	78	4.25
25	76	F	21.42	Melanoma	Rt. sole	Rt. inguinal	1309	78	3.58
26	85	F	19.61	Melanoma	Rt. hallux	Rt. inguinal	916	66	4.32
27	89	F	18.62	Melanoma	Rt. hallux	Rt. inguinal	900	65	4.33
28	74	F	22.31	Melanoma	Rt. hallux	Rt. inguinal	888	63	4.26

BMI, body mass index, which is the height/weight ratio, calculated by body weight (kg) divided by the square of the height (m); M, male; F, female; SST, scintigraphic saturation time; SCC, squamous cell carcinoma; AGC, apocrine adenocarcinoma; EMP, extramammary Paget's disease.

**Table 2.** Clinical profile of patients with nodal metastasis

Case	Age (years)	Sex	BMI	Tumor	Location	Site of Sentinel lymph node	SST (sec)	Distance (cm)	Lymphatic transit rate (cm/min)
29	52	M	23.97	Melanoma	Rt. anterior chest	Rt. axillary	653	28	2.57
30	71	M	26.63	Melanoma	Rt. back	Rt. axillary	165	13	4.73
31	82	F	24.20	MCC	Rt. buttock	Lt. inguinal	214	10	2.80
32	56	F	18.47	EPC	Rt. sole	Rt. inguinal	833	80	5.76
33	21	F	19.55	Melanoma	Rt. lateral knee	Rt. Inguinal	470	38	4.85

BMI, body mass index, which is the height/weight ratio, calculated by body weight (kg) divided by the square of the height (m); M, male; F, female; SST, scintigraphic saturation time; MCC, Merkel cell carcinoma; EPC, eccrine porocarcinoma.

entry of the radionuclide into the subcapsular sinus of the SLN until the entire lymph node is visible on the computer screen of the gamma camera is unknown.

In our institute, the time-activity curve of the lower limbs was used to assess lymph function using dynamic lymphoscintigraphy.<sup>14</sup> In the lower limb, where the radionuclide was

injected into the foot and the time-activity curves of the knee and groin were created, the time at which the counts rose was determined to be the SAT.<sup>14</sup>

In cases in which the SLNs are located at a distance from the primary focus, we could determine the time at which the counts rose as the SAT. However, in cases in which the SLNs

**Table 3.** Lymphatic transit rates in clinical characteristics of negative sentinel nodes

Characteristics	Mean lymphatic transit rate (cm/min)			
	Head and neck (n = 7)	Trunk (n = 9)	Upper limb (n = 6)	Lower limb (n = 9)
Age				
<70	1.23 (n = 4)	1.76 (n = 5)	2.68 (n = 3)	3.97 (n = 4)
≥70	1.03 (n = 3)	1.83 (n = 4)	2.67 (n = 3)	4.17 (n = 5)
Sex				
Male	1.16 (n = 4)	1.62 (n = 6)	2.75 (n = 3)	4.23 (n = 2)
Female	1.11 (n = 3)	2.12 (n = 3)	2.59 (n = 3)	4.02 (n = 7)
BMI				
<23	1.36 (n = 3)	1.95 (n = 4)	2.80 (n = 2)	4.14 (n = 7)
≥23	0.98 (n = 4)	1.66 (n = 5)	2.61 (n = 4)	3.81 (n = 2)

BMI, body mass index, which is the height/weight ratio, calculated by body weight (kg) divided by the square of the height (m).

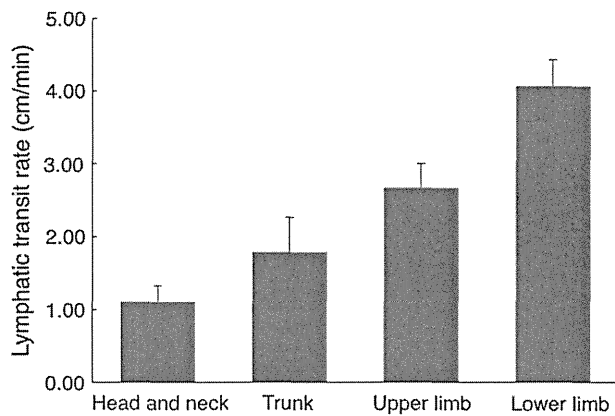


**Figure 3.** Lymphatic transit rates of the various parts of the human body.

are close to the primary focus, there was some accumulation of tracer counts in the initial phase, and it was difficult to determine the time at which the counts rose. In such cases, radionuclide in the syringe and injection sites may influence the counts of the initial measurement (Figs 1, 2). Therefore, in the present method, we did not determine the SAT time at which the counts rose, but newly defined the SST as the point at which the counts reached a plateau as an alternative to the conventional SAT.

We speculated that the time at which the counts reach the plateau is the moment at which the SLN is filled with radioisotope and at which the inflow and outflow of radioisotope in the SLN becomes balanced. Our method may more accurately detect the time than does conventional SLN visualization.

Nathanson *et al.*<sup>1</sup> reported that the rate of lymphatic flow to the axillary, inguinal, popliteal, and parotid SLNs averaged

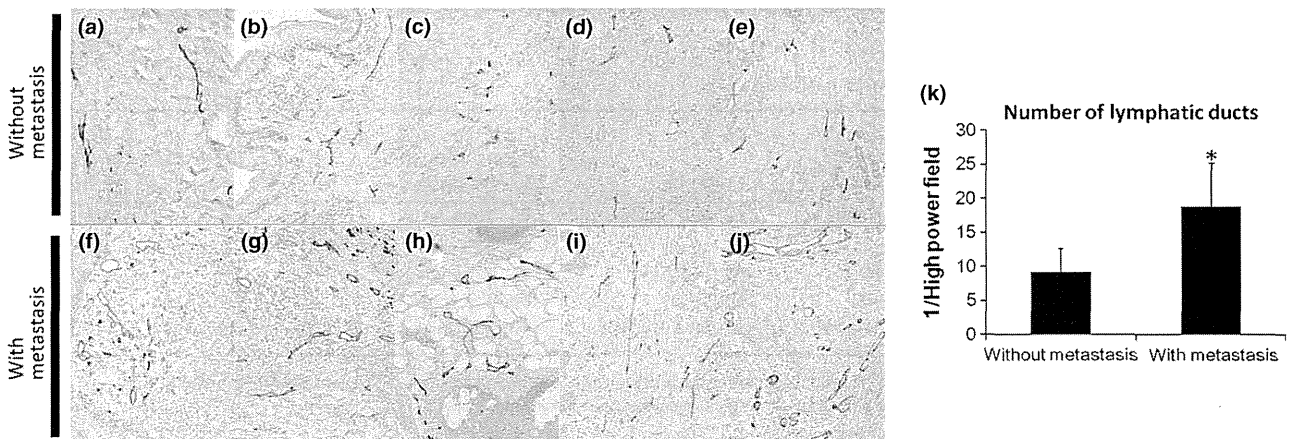


**Figure 4.** Immunostaining of the peritumoral area for D2-40 (original magnification, ×100), a typical lymphatic duct marker, and counted number of lymphatic ducts in patients with metastasis to lymph nodes (n = 5) and in patients without metastasis (n = 5). (a) Case 7, squamous cell carcinoma. (b) Case 9, Paget’s cancer. (c) Case 10, melanoma. (d) Case 20, melanoma. (e) Case 21, melanoma. (f) Case 29, melanoma. (g) Case 30, melanoma. (h) Case 31, Merkel cell cancer. (i) Case 32, eccrine porocarcinoma. (j) Case 33, melanoma. Higher numbers of dilated lymphatic ducts were observed in cases with lymph node metastasis (f–j) than in cases without metastasis (a–e). (k, mean value ± standard deviation, \*P < 0.05 versus cases without metastasis, unpaired Student’s *t*-test).

10.4 ± 7.3 cm/min using <sup>99m</sup>Tc-labeled human serum albumin. On the other hand, Uren *et al.*<sup>2</sup> stated that the lymphatic flow rate is not uniform throughout the body and varies systemically from different areas of the skin. The mean lymphatic flow rate was 5.8 cm/min for the lower limb, 3.1 cm/min for the forearm, 2.6 cm/min for the posterior trunk, 2.3 cm/min for the anterior trunk, and 1.5 cm/min for the head and neck. Like Uren *et al.*, we observed major differences in LTRs from the skin of different parts of the body.

In previous reports, the radioisotopes used in lymphoscintigraphy varied. The particle size of <sup>99m</sup>Tc-phytate is relatively large compared with that of other radioisotope tracers used in previous reports. Although the LTR in our method was slightly slower than the lymphatic flow rate of Uren *et al.*<sup>2,3,12</sup> because of this larger particle size, our results are similar to those obtained by Uren *et al.* This may prove the validity of lymphatic flow measurement using <sup>99m</sup>Tc-phytate.

Some recent reports have aimed to determine whether the SAT of the SLN, as determined by lymphoscintigraphy, has prognostic value in predicting metastasis dissemination in patients with cutaneous malignant melanoma.<sup>8–10</sup> No patients with an SAT of >30 min had positive SLNs, and all patients with positive SLNs had an SAT of <30 min.<sup>8–10</sup> As the radioisotope tracer, they used <sup>99m</sup>Tc-nanocolloid or <sup>99m</sup>Tc-colloidal rhenium sulfide, the particle sizes of which are smaller than that of <sup>99m</sup>Tc-phytate.<sup>8–10</sup> All SSTs were within 30 min in our series in spite of the large particle size. This may have been because our method quickly captured the moment at which the SLN was filled with radioisotope.

Physiologically, factors such as the volume of lymph produced per unit of time (which can be higher in the limbs because of gravitational effects on hydrostatic pressure within the blood capillaries), mechanical pump effects caused by skeletal muscle contractions, intrinsic rhythmic pulsation of the lymph vessels, and temperature influence the amount of lymphatic flow.<sup>8</sup> With respect to aging, Conway *et al.*<sup>15</sup> described that lymphatic function, as assessed by radiocolloid transit to, and uptake within, the SLN declines with age. However, a correlation between age and LTR was not demonstrated in the present study. Ogasawara *et al.*<sup>16</sup> reported that in the SLN biopsies of patients with breast cancer, a significant correlation was seen between BMI and the transit time to the axilla after subdermal dye injection using fluorescence imaging. They elucidated that the diffusion rate of the dye might be lower and the lymphatic flow slower in more obese patients.<sup>16</sup> Similarly, in the present cases, the mean LTRs were lower in patients with a BMI of ≥23 than in patients with a BMI of <23.

Pathologically, induction of lymphangiogenesis by cytokines that are secreted by tumor cells affects the lymphatic vessel density and lumen diameter.<sup>17</sup> Previous studies have shown that the peritumoral lymphatic vessel density is increased in patients with melanoma, and the lymphatic vessel lumen diameter has been shown to be increased in mice with melanoma.<sup>4,18,19</sup> SST might be influenced not only by the rate of lymphatic flow, but also to some degree by the peritumoral lymphatic vessel density and lumen diameter. In the present

study, the peritumoral lymphatic vessel density was substantially higher in patients with nodal metastasis than in patients without nodal metastasis (Fig. 4). This may suggest that an increase in the peritumoral lymphatic vessel density contributes to nodal metastasis.

The area extraction method may allow for more accurate measurement of the SAT and lymphatic flow rate. Further studies of larger numbers of patients will be required to confirm that the SAT and lymphatic flow rate of the SLN are important predictive parameters of metastatic disease in SLNs because the number of patients with positive SLNs was small in this report.

**ACKNOWLEDGMENT:** This work was supported in part by a Grant-in-Aid for Scientific Research (C) from the Japan Society for the Promotion of Science (JSPS; No. 24591625).

**CONFLICTS OF INTEREST:** None.

## REFERENCES

- Nathanson SD, Nelson L, Karvelis KC. Rates of flow of technetium 99 m-labeled human serum albumin from peripheral injection sites to sentinel lymph nodes. *Ann Surg Oncol* 1996; **3**: 329–335.
- Uren RF, Hawman-Giles R, Thompson JF. Variation in cutaneous lymphatic flow rates. *Ann Surg Oncol* 1997; **4**: 279–281.
- Uren RF, Howman-Giles RB, Thompson JF, Roberts J, Bernard E. Variability of cutaneous lymphatic flow rates in melanoma patients. *Melanoma Res* 1998; **8**: 279–282.
- Nathanson SD, Anaya P, Avery M, Hetzel FW, Sarantou T, Havstad S. Sentinel lymph node metastasis in experimental melanoma: relationships among primary tumor size, lymphatic vessel diameter and <sup>99m</sup>Tc-labeled human serum albumin clearance. *Ann Surg Oncol* 1997; **4**: 161–168.
- Harrell MI, Iritani BM, Ruddell A. Tumor-induced sentinel lymph node lymphangiogenesis and increased lymph flow precede melanoma metastasis. *Am J Pathol* 2007; **170**: 774–786.
- Ruddell A, Harrell MI, Minoshima S *et al.* Dynamic contrast-enhanced magnetic resonance imaging of tumor-induced lymph flow. *Neoplasia* 2008; **10**: 706–713, 1 p following 713.
- Maza S, Valencia R, Geworski L *et al.* Influence of fast lymphatic drainage on metastatic spread in cutaneous malignant melanoma: a prospective feasibility study. *Eur J Nucl Med Mol Imaging* 2003; **30**: 538–544.
- Cammilleri S, Jacob T, Rojat-Habib MC *et al.* High negative predictive value of slow lymphatic drainage on metastatic node spread detection in malignant limb and trunk cutaneous melanoma. *Bull Cancer* 2004; **91**: E225–E228.
- Mahieu-Renard L, Cammilleri S, Giorgi R *et al.* Slow dynamics of lymphoscintigraphic mapping is associated to the negativity of the sentinel node in melanoma patients. *Ann Surg Oncol* 2008; **15**: 2878–2886.
- Richtig E, Komericki P, Trapp M *et al.* Ratio of marked and excised sentinel lymph nodes and scintigraphic appearance time in melanoma patients with negative sentinel lymph node. *Eur J Surg Oncol* 2010; **36**: 783–788.
- Akhras V, Stanton AW, Levick JR, Mortimer PS. A quantitative examination of lymph drainage from perilesion skin in human melanoma. *Lymphat Res Biol* 2012; **10**: 107–111.
- Uren RF, Howman-Giles RB, Chung D, Thompson JF. Role of lymphoscintigraphy for selective sentinel lymphadenectomy. *Cancer Treat Res* 2005; **127**: 15–38.

- 13 Fujiwara M, Mizukami T, Suzuki A, Fukamizu H. Sentinel lymph node detection in skin cancer patients using real-time fluorescence navigation with indocyanine green: preliminary experience. *J Plast Reconstr Aesthet Surg* 2009; **62**: e373–e378.
- 14 Unno N, Nishiyama M, Suzuki M *et al.* Quantitative lymph imaging for assessment of lymph function using indocyanine green fluorescence lymphography. *Eur J Vasc Endovasc Surg* 2008; **36**: 230–236.
- 15 Conway WC, Faries MB, Nicholl MB *et al.* Age-related lymphatic dysfunction in melanoma patients. *Ann Surg Oncol* 2009; **16**: 1548–1552.
- 16 Ogasawara Y, Ikeda H, Takahashi M, Kawasaki K, Doihara H. Evaluation of breast lymphatic pathways with indocyanine green fluorescence imaging in patients with breast cancer. *World J Surg* 2008; **32**: 1924–1929.
- 17 Nathanson SD. Insights into the mechanisms of lymph node metastasis. *Cancer* 2003; **98**: 413–423.
- 18 Shields JD, Borsetti M, Rigby H *et al.* Lymphatic density and metastatic spread in human malignant melanoma. *Br J Cancer* 2004; **90**: 693–700.
- 19 Dadras SS, Lange-Asschenfeldt B, Velasco P *et al.* Tumor lymphangiogenesis predicts melanoma metastasis to sentinel lymph nodes. *Mod Pathol* 2005; **18**: 1232–1242.

# IL-23 from Langerhans Cells Is Required for the Development of Imiquimod-Induced Psoriasis-Like Dermatitis by Induction of IL-17A-Producing $\gamma\delta$ T Cells

Ryutaro Yoshiki<sup>1</sup>, Kenji Kabashima<sup>2</sup>, Tetsuya Honda<sup>2</sup>, Satoshi Nakamizo<sup>2</sup>, Yu Sawada<sup>2</sup>, Kazunari Sugita<sup>1</sup>, Haruna Yoshioka<sup>1</sup>, Shun Ohmori<sup>1</sup>, Bernard Malissen<sup>3</sup>, Yoshiki Tokura<sup>4</sup> and Motonobu Nakamura<sup>1</sup>

Psoriasis is a common chronic inflammatory skin disease that involves dysregulated interplay between immune cells and keratinocytes. Recently, it has been reported that IL-23 induces CCR6<sup>+</sup>  $\gamma\delta$  T cells, which have the pivotal role in psoriasis-like skin inflammation in mice of producing IL-17A and IL-22. Langerhans cells (LCs) are a subset of dendritic cells that reside in the epidermis and regulate immune responses. The role of LCs has been extensively investigated in contact hypersensitivity, but their role in psoriasis remains to be clarified. In this study, we focused on Th17-related factors and assessed the role of LCs and  $\gamma\delta$  T cells in the development of psoriasis using a mouse psoriasis model triggered by topical application of imiquimod (IMQ). LC depletion by means of diphtheria toxin (DT) in Langerin DT receptor-knocked-in mice suppressed hyperkeratosis, parakeratosis, and ear swelling in the IMQ-treated regions. In addition, LC-depleted mice showed decreased levels of Th17-related cytokines in IMQ-treated skin lesions. Moreover, the IMQ-treated skin of LC-depleted mice showed a decreased number of IL-17A-producing CCR6<sup>+</sup>  $\gamma\delta$  T cells. These results suggest that LCs are required for the development of psoriasis-like lesions induced by IMQ in mice.

*Journal of Investigative Dermatology* (2014) 134, 1912–1921; doi:10.1038/jid.2014.98; published online 3 April 2014

## INTRODUCTION

Psoriasis is an inflammatory epidermal hyperproliferative skin disease that affects 2–3% of the population in Caucasians. In this disease, patients develop erythematous papules and scaly plaques over the skin surface. Several lines of evidence, such as the presence of activated CD4<sup>+</sup> and CD8<sup>+</sup> T cells in psoriatic plaques (Ferenczi *et al.*, 2000), the results of studies on human skin xenografts in mice (Boyman *et al.*, 2004), and the therapeutic efficacy of T cell-targeted drugs (Di Cesare *et al.*, 2009), have suggested the involvement of T cell-

mediated immune responses in this disease. In addition, the expression levels of IL-1, tumor necrosis factor (TNF), IL-12, IL-17, IL-22, and IL-23 are elevated in psoriatic skin in humans (Di Cesare *et al.*, 2009), and IL-23R gene polymorphisms are associated with psoriasis (Capon *et al.*, 2007). These findings suggest the involvement of these cytokines in the pathogenesis of this skin disease.

Recent studies have demonstrated that the IL-23/Th17 pathway is linked to a number of inflammatory diseases, including psoriasis and animal models of multiple sclerosis, arthritis, and inflammatory bowel disease (Cua *et al.*, 2003). The most persuasive evidence for the role of IL-23/Th17 in psoriasis comes from clinical studies. Treatment with an anti-IL-12/IL-23p40 Ab (ustekinumab) is effective against psoriasis (Krueger *et al.*, 2007). TNF- $\alpha$ -neutralizing antibodies are also widely used to treat psoriasis and significantly improve psoriasis area severity index scores. Notably, inhibition of TNF- $\alpha$  by a soluble TNF- $\alpha$  receptor-neutralizing antibody (etanercept) was associated with reduced Th17 responses (Zaba *et al.*, 2007). As Th1 responses were not affected by the administration of etanercept, this finding suggests that Th17 cells are particularly important in driving psoriasis. Consistently, amelioration of psoriasis has been associated with reduced Th17 responses (Zaba *et al.*, 2007). Th17 cytokines, principally IL-17A and IL-22, exert profound effects on keratinocytes (Nogales *et al.*, 2008). In psoriasis lesions, keratinocytes are activated and proliferate at

<sup>1</sup>Department of Dermatology, University of Occupational and Environmental Health, Kitakyushu, Japan; <sup>2</sup>Department of Dermatology, Kyoto University, Kyoto, Japan; <sup>3</sup>Centre d'Immunologie de Marseille-Luminy, Institut National de la Santé et de la Recherche Médicale U631, Centre National de la Recherche Scientifique UMR6102, Université de la Méditerranée, Marseille, France and <sup>4</sup>Department of Dermatology, Hamamatsu University School of Medicine, Hamamatsu, Japan

Correspondence: Ryutaro Yoshiki, Department of Dermatology, University of Occupational and Environmental Health, 1-1 Iseigaoka, Kitakyushu 807-8555, Japan. E-mail: yockey@med.uoeh-u.ac.jp or Kenji Kabashima, Department of Dermatology, Kyoto University Graduate School of Medicine, 54 Shogoin-Kawara, Kyoto 606-8507, Japan. E-mail: kaba@kuhp.kyoto-u.ac.jp

Abbreviations: dDCs, dermal dendritic cells; DT, diphtheria toxin; IMQ, imiquimod; LCs, Langerhans cells; TLR, Toll-like receptor; TNF, tumor necrosis factor

Received 12 December 2012; revised 26 December 2013; accepted 7 January 2014; accepted article preview online 25 February 2014; published online 3 April 2014



substantially faster rates than normal keratinocytes (Iizuka, 1994). IL-17A has been shown to induce cytokine and chemokine production by keratinocytes, whereas IL-22 induces antimicrobial peptide production by keratinocytes and is a direct potent stimulator of keratinocyte growth (Nogales *et al.*, 2008).

More recently, topical treatment with imiquimod (IMQ), a ligand for Toll-like receptor (TLR) 7 and TLR8, was reported as a novel mouse model for psoriasis-like skin inflammation inducing acanthosis, parakeratosis, and a mixed inflammatory infiltrate (van der Fits *et al.*, 2009). IMQ is used in humans for topical treatment of genital and perianal warts caused by human papillomavirus, actinic keratosis, and superficial basal cell carcinoma. Clinical application of IMQ can induce psoriasis or exacerbate the disease in patients with well-controlled psoriasis (Fanti *et al.*, 2006). In mice, IMQ-induced dermatitis development is critically dependent on the IL-23/IL-17 axis (van der Fits *et al.*, 2009). Moreover, administration of IL-23 into mouse skin results in the epidermal recruitment of CCR6<sup>+</sup> cells, a subtype of  $\gamma\delta$  T cells that produces IL-17A (Mabuchi *et al.*, 2011), and IMQ-treated mice show increased numbers of IL-17-producing  $\gamma\delta$  T cells (Roller *et al.*, 2012). However, it remains unclear how these IL-17-producing  $\gamma\delta$  T cells are induced in the IMQ-treated skin, specifically in regard to the involvement of skin resident-dendritic cells (DCs).

Recent immunological studies have demonstrated that there are Langerhans cells (LCs), Langerin<sup>-</sup> dermal DCs (dDCs), and Langerin<sup>+</sup> dDCs in murine skin (Ginhoux *et al.*, 2007). LCs are a subset of skin-resident DCs that form a dense network in the epidermis (Romani *et al.*, 2010; Egawa and Kabashima, 2011). The role of LCs has been well studied in contact hypersensitivity, the induction of which is a classical technique permitting the examination of cutaneous adaptive immune responses (Honda *et al.*, 2012; Kaplan *et al.*, 2012). Transgenic mice with an inducible or constitutive ablation of LCs showed enhanced contact hypersensitivity (Kaplan *et al.*, 2005), whereas other LC ablation mouse models developed reduced or unaffected contact hypersensitivity (Bennett *et al.*, 2007).

In this study, we explored the role of LCs in a mouse model in which psoriasis-like skin inflammation is triggered by topical application of IMQ. LC-depleted mice showed reduced ear swelling and decreased levels of Th17-related cytokines in IMQ-treated skin regions. LC-depleted IMQ-treated skin showed decreased IL-17A production and expression of CCR6 from skin  $\gamma\delta$  T cells. We also found that LCs produce IL-23 in IMQ-applied skin regions and that IL-23-producing cells were reduced at draining lymph nodes after IMQ application. These results suggest that LCs are required for generation of psoriasis-like lesions in response to IMQ in mouse models.

## RESULTS

### LC-depleted mice show reduced IMQ-induced psoriasis-like skin inflammation

Consistent with a previous report (van der Fits *et al.*, 2009), topical application of IMQ on the skin of wild-type mice for 5 days induced psoriasis-like lesions featuring redness, scales,

and crust formation. To evaluate the function of LCs in the pathogenesis of psoriasis, LCs were depleted with diphtheria toxin (DT) in Langerin-DT receptor (DTR)-knocked-in mice. LCs were completely ablated from the epidermis within 24 h after injection of DT. We also investigated whether Langerin<sup>+</sup> dDCs are involved in IMQ-induced psoriasis-like skin inflammation. It has been reported that Langerin<sup>+</sup> dDCs recolonize in the dermis in 5 days or less after DT injection (Bursch *et al.*, 2007). Ten days after DT injection, LCs are still absent in the epidermis but dDCs are present (Supplementary Figure 1a online). IMQ cream was applied on both ears of LC/Langerin<sup>+</sup> dDC-depleted mice or on ears of LC-depleted mice for 5 consecutive days. When the absolute number of each LC/DC subset per skin specimen was calculated, the subset of Langerin<sup>+</sup> dDCs absolutely disappeared by IMQ application, but that of LCs and Langerin<sup>-</sup> dDCs was not affected (Supplementary Figure 1a, b, d, e, f online). In addition, the IMQ application increased the number of Gr1<sup>+</sup> cells regardless of the depletion of LCs or Langerin<sup>+</sup> dDCs (Supplementary Figure 1c, g online). Ear thickness was measured on day 6 after the start of IMQ application. Compared with IMQ-treated non-DT control mice, LC-depleted and IMQ-treated mice showed milder increases in ear thickness (Figure 1a and b). To exclude the involvement of newly differentiated LCs, we applied a daily DT treatment and IMQ application for 5 consecutive days to ensure efficient ablation of LC throughout the course of disease. A daily DT treatment and IMQ application did not affect the result of the ear thickness change (Supplementary Figure 2 online). Microscopic evaluation of skin sections from mice treated with IMQ revealed changes characteristic of psoriasis-like lesions, such as acanthosis, parakeratosis, desquamation, and dermal infiltration of immune cells. In contrast, IMQ administration had qualitatively and quantitatively fewer effects on Langerin<sup>+</sup> cell (including LCs and Langerin<sup>+</sup> dDCs)-depleted mice (IMQ application 1 day after DT treatment; Day 1) or LC-depleted mice (IMQ application 10 days after DT treatment; Day 10) (Figure 1a). Hyperproliferation of keratinocytes in IMQ-induced psoriatic regions was also monitored by immunohistochemical staining of Stat3 and Ki67. IMQ-treated skin keratinocytes of control C57BL/6 mice were highly positive for Stat3 and Ki67 as compared with IMQ-treated Langerin<sup>+</sup> cell-depleted (Day 1) or LC-depleted mice (Day 10) (Figure 1a and c). These findings indicate that LCs are critical for the induction of IMQ-induced psoriasis-skin inflammation.

### LC-depleted skin shows decreased IL-12/23p19, IL-12/23p40, IL-17A, IL-22, and TNF- $\alpha$ mRNA induction by IMQ

Recently, the roles of Th1 and Th17 cytokines in the pathogenesis of IMQ-induced psoriasis-like skin inflammation have been demonstrated (van der Fits *et al.*, 2009). To characterize immune responses in IMQ-treated skin of LC-depleted mice, the expression of cytokines was measured by real-time PCR. IMQ cream was applied on both ears of LC/Langerin<sup>+</sup> dDC-depleted mice or only LC-depleted mice for 5 consecutive days. On day 6, the mice were killed and mRNA from both ears was extracted. In control C57BL/6J mice,

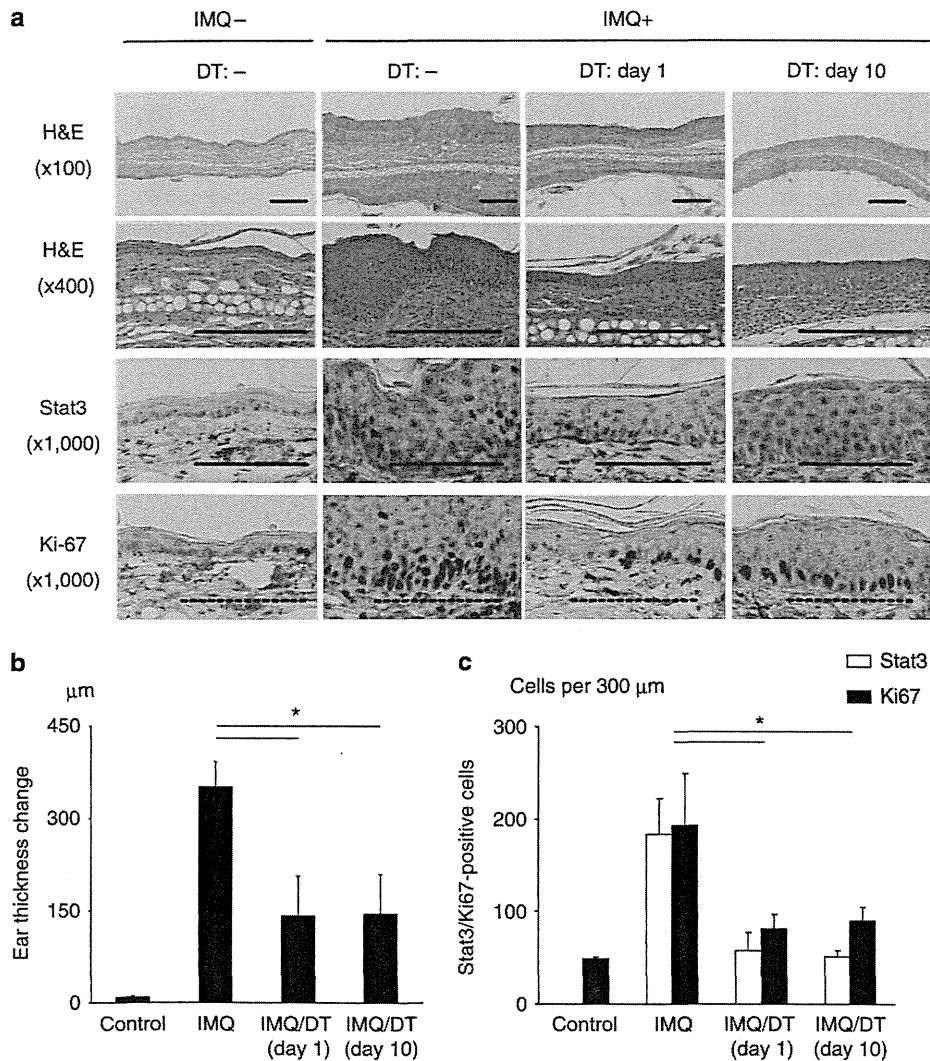


**Figure 1.** Langerhans cell-depleted mice show decreased IMQ-induced psoriasis-like skin inflammation. Langerin<sup>+</sup> cells were depleted by DT in Langerin-DTR-knocked-in mice. Langerin<sup>+</sup> dDCs, but not Langerhans cells, repopulated in the skin 10 days later. C57BL/6J mice or Langerin-DTR-knocked-in mice were treated daily with IMQ cream or control cream application on both ears for 5 consecutive days. (a) H&E-stained and immunohistochemical staining of Stat3, Ki-67 sections. (b) The ear swelling at day 6. (c) The numbers of Stat3- or Ki67-positive keratinocytes. Data are representative of four independent experiments and each group consisted of more than four mice. \**P*<0.05 between indicated groups. Normal bar = 200 μm, dotted bar = 100 μm. dDCs, dermal dendritic cells; DT, diphtheria toxin; DTR, DT receptor; H&E, hematoxylin and eosin; IMQ, imiquimod.

application of IMQ induced IL-12/23p19, IL-12/23p40, IL-17A, IL-22, and TNF- $\alpha$  mRNA expression (Figure 2a–e), whereas expression of IL-12p35 mRNA was not detected by real-time PCR (data not shown). In LC-depleted and IMQ-treated mice, the induction of IL-12/23p19, IL-12/23p40, IL-17A, IL-22, and TNF- $\alpha$  mRNAs was suppressed on both day 1 and day 10 (Figure 2a–e). As IL-23 maintains IL-17-producing cells, the above findings suggest that IMQ stimulates the production of IL-23, but not of IL-12, in LCs, which in turn promotes Th17 in IMQ-treated skin lesions.

**IMQ induces IL-23 production from LCs after application of IMQ**  
Recently, it was postulated that IL-23, a cytokine driving the development of IL-17- and IL-22-producing Th17 cells, is

functionally involved in the pathogenesis of psoriasis. Expression of IL-23 is increased in psoriasis lesional skin (Lee *et al.*, 2004), and increased numbers of Th17 cells are present (Lowes *et al.*, 2008). Application of IMQ leads to hyperplasia of the epidermis. In the same fashion, intradermal injection of IL-23 in mouse skin results in erythema, a mixed inflammatory infiltrate, and epidermal hyperplasia (Chan *et al.*, 2006). However, the source of IL-23 in psoriasis is still unclear. To investigate the source of IL-23 in IMQ-treated psoriasis-like skin, we first examined the expression of TLR7, a receptor for IMQ, in the skin-composing cells. In the steady state, LCs and Langerin<sup>+</sup> and Langerin<sup>-</sup> dDCs expressed TLR7, whereas  $\gamma\delta$  T cells, Gr1<sup>+</sup> cells, and keratinocytes were TLR7 negative irrespective of IMQ application (Figure 3a and b). Recently, it has been reported that the IMQ-containing

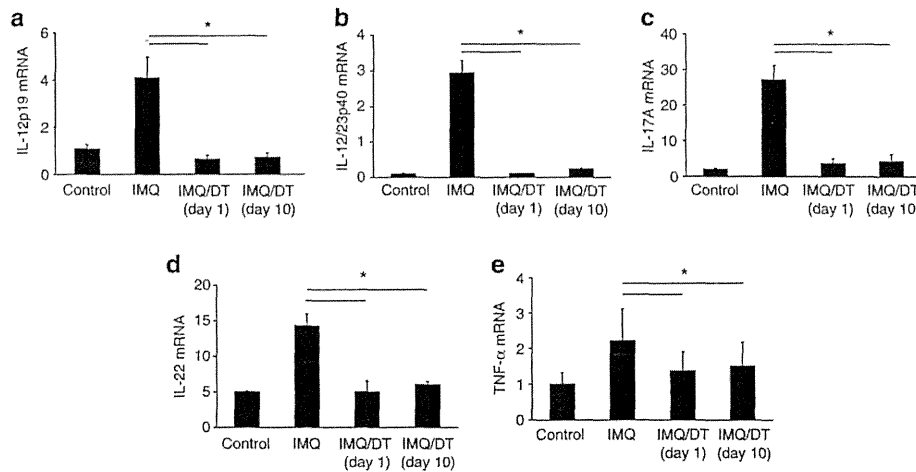


Figure 2. IMQ application induces cytokine mRNA production in skin. IMQ cream was applied on both ears of LC/Langerin<sup>+</sup> d DC-depleted mice or LC-depleted mice for 5 consecutive days. Real-time PCR analysis revealed that LC-depleted skin showed less expression of (a) IL-12p19, (b) IL-12/23p40, (c) IL-17A, (d) IL-22, and (e) TNF- $\alpha$  mRNA after IMQ application. Error bars indicate s.d. based on a single, pooled treatment group that was divided into three wells for RT-PCR measurement. Similar results were obtained in two independent experiments and each group consisted of more than four mice. \* $P < 0.05$  between indicated groups. DC, dendritic cell; DT, diphtheria toxin; IMQ, imiquimod; LC, Langerhans cell; TNF, tumor necrosis factor.

cream 'Aldara' induces inflammation largely independently of TLR7 and vehicle cream also promotes inflammasome activation in cultured keratinocytes (Walter *et al.*, 2013). To examine whether IMQ affects the expression of TLR7 to skin containing cells, we measured the TLR7-mRNA expression by real-time PCR. LCs,  $\gamma\delta$  T cells, and KCs showed no remarkable change of TLR7-mRNA; however, only Langerin<sup>-</sup> dDCs showed high expression of TLR7-mRNA (Figure 3c). As shown in Supplementary Figure 1b online, Langerin<sup>+</sup> dDCs disappeared from IMQ-applied skin and expression of TLR7 from Langerin<sup>+</sup> dDCs could not be measured. We next examined the IL-23-producing cells in the IMQ-applied skin by means of flow cytometry. IMQ-applied skin contained more IL-23-producing cells than did control mice (Figure 3d and e). To identify which cells produced IL-23, IMQ applied skins were analyzed by flow cytometry stained by EpCAM, Langerin,  $\gamma\delta$ TCR, and Gr1. Only both EpCAM- and Langerin-positive cells or LCs produced IL-23 after IMQ application to the skin (Figure 3f). In control skin,  $\sim 10\%$  or less of LCs produce IL-23. However,  $\sim 80\%$  of LCs produced IL-23 in IMQ-applied skin (Figure 3g). These results suggest that IMQ administration induces IL-23 production in LCs.

#### Decreased infiltration of IL-17A-producing CCR6<sup>+</sup> $\gamma\delta$ T cells in LC-depleted skin after IMQ application

It has been reported that IL-23-responsive dermal  $\gamma\delta$  T cells are the major IL-17 producers in the skin (Cai *et al.*, 2011), and were revealed to express CCR6 in a murine model of psoriasis (Mabuchi *et al.*, 2011). We next investigated the production of IL-17A and CCR6 expression from  $\gamma\delta$  T cells in IMQ-treated skin. IMQ cream was applied on both ears of LC/Langerin<sup>+</sup> dDC-depleted mice or on ears of only LC-depleted mice for 5 consecutive days. On day 6, epidermal-cell and dermal-cell suspensions were prepared from IMQ-treated skin. When IMQ was applied to non-DT-treated mice, increased

numbers of IL-17A-producing  $\gamma\delta$ TCR mid<sup>+</sup> T cells were detected in the epidermis, which were reduced in LC-depleted mice (Figure 4a and b). On the other hand, similar numbers of IL-17A-producing  $\gamma\delta$ TCR mid<sup>+</sup> cells were observed in the dermis of IMQ-treated skin regardless of the presence of LCs (Figure 4c and d). These IL-17A-producing  $\gamma\delta$ TCR mid<sup>+</sup> cells were V $\gamma$ 4 and CCR6 positive (Supplementary Figure 3 online). We also analyzed the IL-17A positive cells in the CD4<sup>+</sup> T-cell subset. The number of IL-17A-producing CD4<sup>+</sup> T cells increased in the IMQ-treated epidermis and dermis. The number of IL-17A-producing CD4<sup>+</sup> cells was decreased in the dermis of LC- or Langerin<sup>+</sup> dDC-depleted skin (Figure 4e-h). These data indicate that LCs induce infiltration of IL 17A-producing CCR6<sup>+</sup>  $\gamma\delta$  TCR mid<sup>+</sup> V $\gamma$ 4<sup>+</sup> cells into epidermis and psoriasis-like inflammation after IMQ application.

#### LC-depleted and IMQ-treated mice show decreased numbers of IL-12/23p40-positive cells and IL-17A-producing $\gamma\delta$ T cells at regional lymph nodes

To analyze IL-23-producing cells and IL-17A-producing cells in the draining lymph nodes, we next performed flow cytometric analysis of regional lymph node cells at the end of a 5-day course of IMQ treatment. Compared with control mice, mice that had just received 5 days of IMQ treatment exhibited increased numbers of IL-23-producing major histocompatibility complex (MHC) class II<sup>+</sup> cells in the draining lymph nodes. On the other hand, Langerin<sup>+</sup> cell-depleted or LC-depleted mice did not show any significant change in the number of IL-23-producing cells (Figure 5a and c). These IL-23-producing MHC class II<sup>+</sup> cells were positive for EpCAM and Langerin, whereas IL-23-non-producing MHC class II<sup>+</sup> cells were negative for EpCAM and Langerin (Figure 5b). Surprisingly, almost all LCs in draining lymph nodes produce IL-23. These results indicate that IL-23-producing MHC class

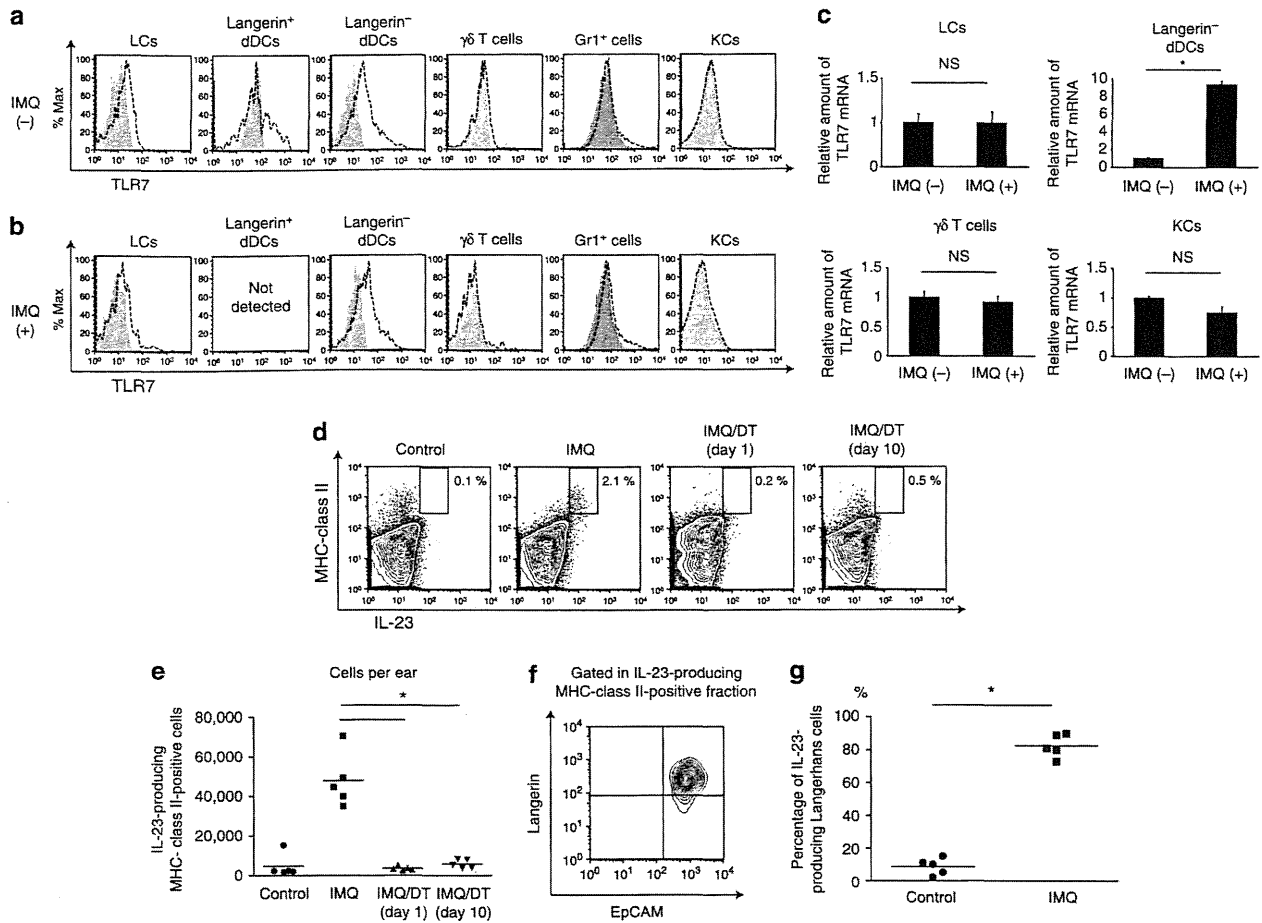


**Figure 3.** LCs produce IL-23 after application of IMQ. IMQ cream was applied to mice ears for 5 consecutive days and whole-skin suspension was analyzed by real-time PCR. (a) TLR7 was expressed on Langerin<sup>-</sup> dDCs by application of IMQ. (b, c) Whole-skin suspension was stained with PE-conjugated IL-23 for flow cytometry. LC-depleted skin did not show an increase in the number of IL-23-producing cells. Data points represent individual frequencies. (d, e) CD4<sup>+</sup> MHC class II-positive cells were gated by EpCAM and Langerin. Other CD45-positive cells were gated by  $\gamma\delta$ TCR and Ly-6G (Gr1). Only LCs showed IL-23 production by IMQ application (f, g). Data are representative of four independent experiments and each group consisted of more than five mice. dDCs, dermal dendritic cells; DT, diphtheria toxin; IMQ, imiquimod; KCs, keratinocytes; LCs, Langerhans cells; MHC, major histocompatibility complex; NS, not significant; TLR, Toll-like receptor.

IL<sup>+</sup> cells are LCs. Similarly, we found that the number of IL-17A-producing  $\gamma\delta$  T cells was significantly increased in the IMQ-treated mice, and decreased in the Langerin<sup>+</sup> cell-depleted or LC-depleted mice (Figure 5d and e). We also studied IL-17A-producing CD4<sup>+</sup> T cells. The number of IL-17A-producing CD4<sup>+</sup> T cells was increased by treatment with IMQ, which was decreased by depletion of Langerin<sup>+</sup> cells or only LCs (Figure 5f and g). Of note, the total number of IL-17A-producing CD4<sup>+</sup> T cells was less than a tenth of IL-17A-producing  $\gamma\delta$  T cells. Thus,  $\gamma\delta$  T cells were the main source of IL-17A in the draining lymph nodes of IMQ-treated mice, and LC abrasion led to reduced numbers of IL-17A-producing  $\gamma\delta$  T cells. These results suggest that LCs are required for the IL-23 pathways that lead to IL-17 production by  $\gamma\delta$  T cells in the draining lymph nodes following IMQ treatment.

#### IL-23 from skin-derived LCs induces psoriatic skin inflammation

On the basis of the indication that IL-23 from LCs may increase IL-17 production by  $\gamma\delta$  T cells in the draining lymph

nodes, we further explored a role of IL-23 from LCs by transplanting bone marrow (BM) cells of IL-23-deficient (IL23KO) mice into X-ray-irradiated wild-type (WT) mice or *vice versa*. As LCs are resistant to X-ray irradiation (Merad *et al.*, 2004), IL-23-producing LCs existed in the skin of X-ray-irradiated WT mice. Two months after transplanting BM cells of WT or IL23KO mice into X-ray-irradiated WT or IL23KO mice, mice received topical applications of commercially available IMQ cream on both ears for 5 consecutive days. Ear thickness was measured on day 6 after the start of IMQ application. Compared with IMQ-treated WT mice in which both donors and recipients were WT, IL23KO mice, in which both donors and recipients were IL23 KO mice, showed a decrease in ear thickness (Figure 6). When transplanting BM cells of WT mice into X-ray-irradiated IL23KO mice ear thickness significantly decreased, whereas ear thickness did not show any change compared with WT mice when transplanting IL23KO BM cells into irradiated WT mice (Figure 6). In Figure 6, WT control showed less swelling than